Cosmological Structure Formation:
From the Big Bang to the Present Day

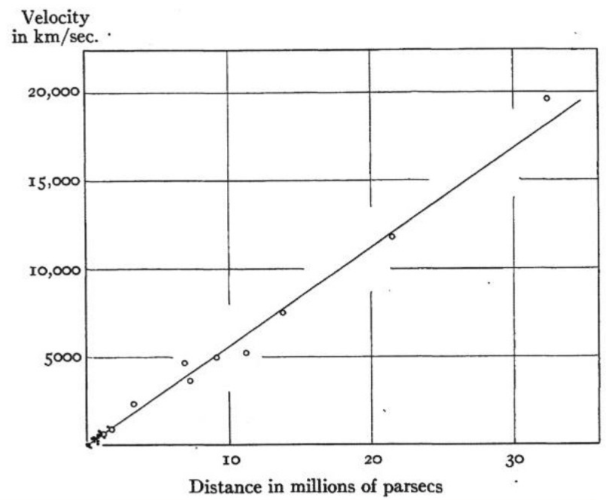

Figure 2: The Hubble law (after Hubble & Humason, 1931: 74).

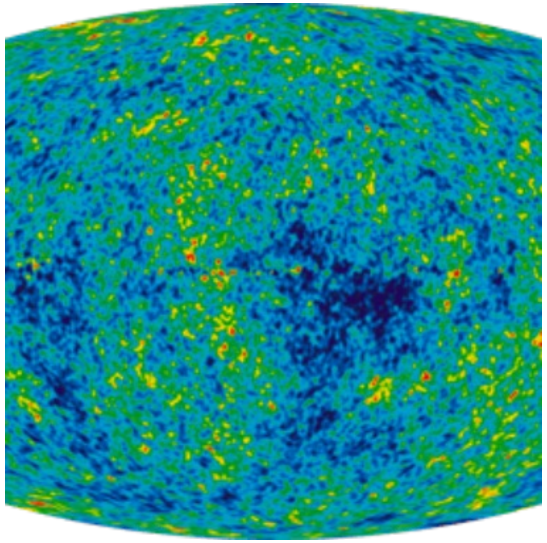

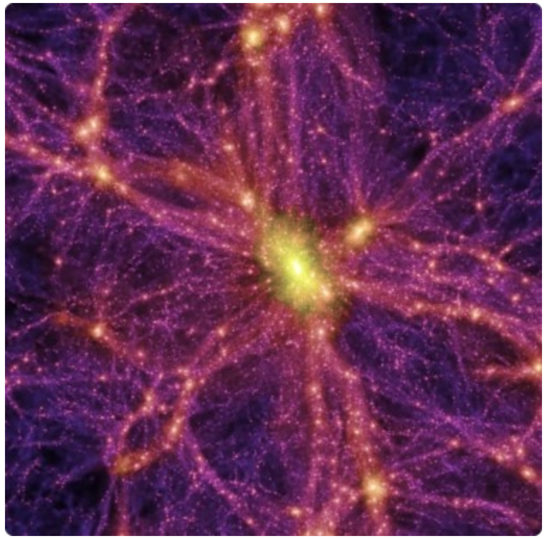

Yong Tian

National Central University

5 July 2023, NCTS-TCA Summer Student Program, Taipei

Standard Cosmology

- Expanding universe
- ΛCDM - accelerating universe with cold dark matter (CDM)
- Bottom-up structure formation
- Galaxies, galaxy clusters, larger cosmic structures
- Challenges

Redshift

$$z = \frac{\lambda_{obs} - \lambda_{emit}}{\lambda_{emit}}$$

$$1 + z = \frac{\lambda_{obs}}{\lambda_{emit}}$$

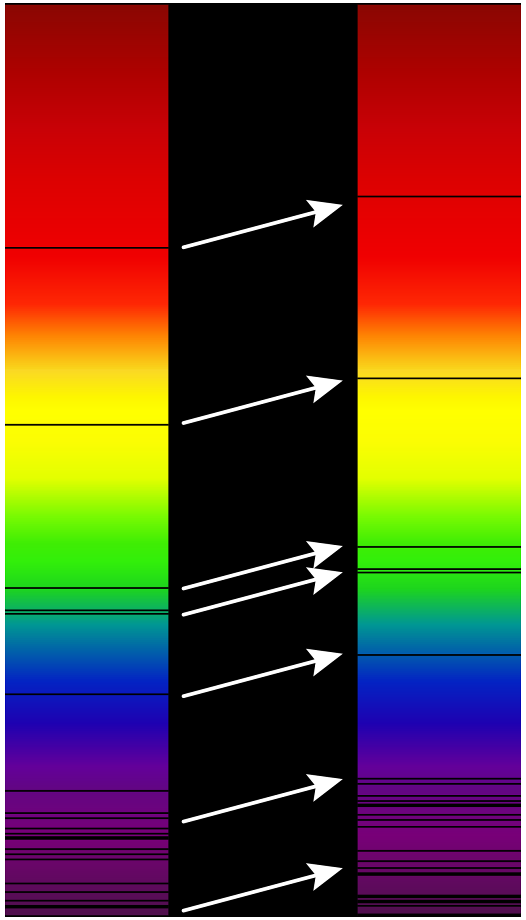

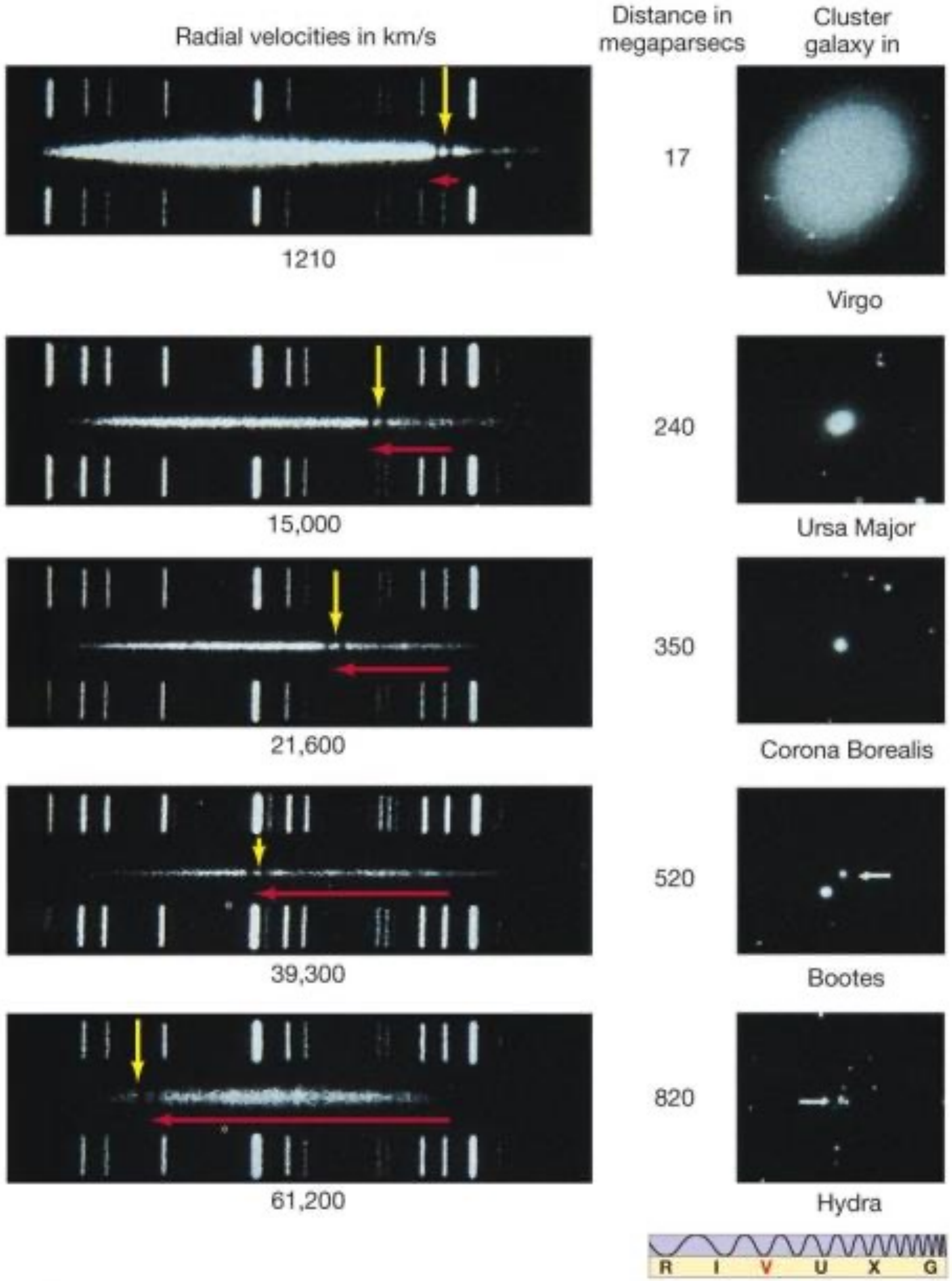

The Possible Origins of the Redshift?

Doppler Effect

The Doppler effect is the shift in the frequency of a wave in relation to an observer due to relative motion of the wave source and observer.

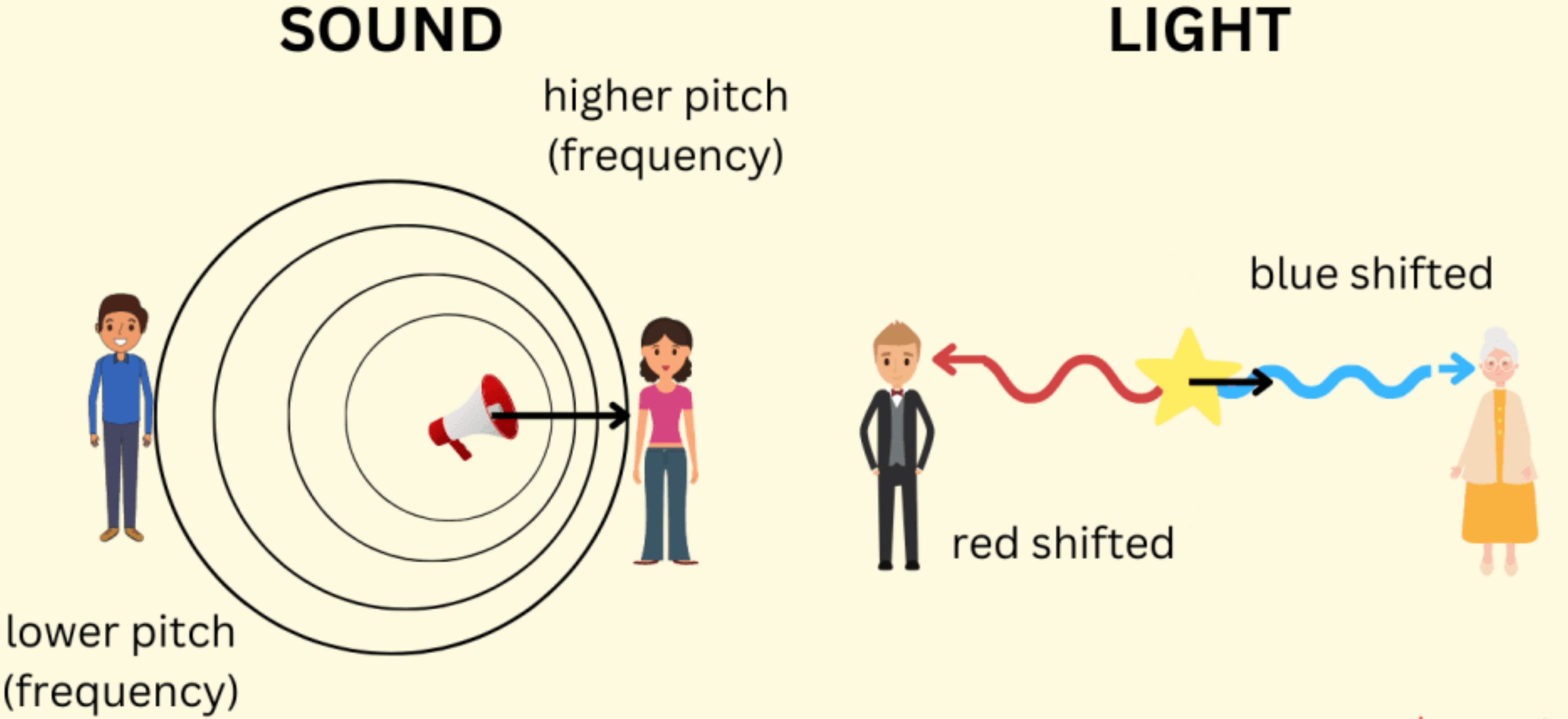

sciencenotes.org

Tired Light

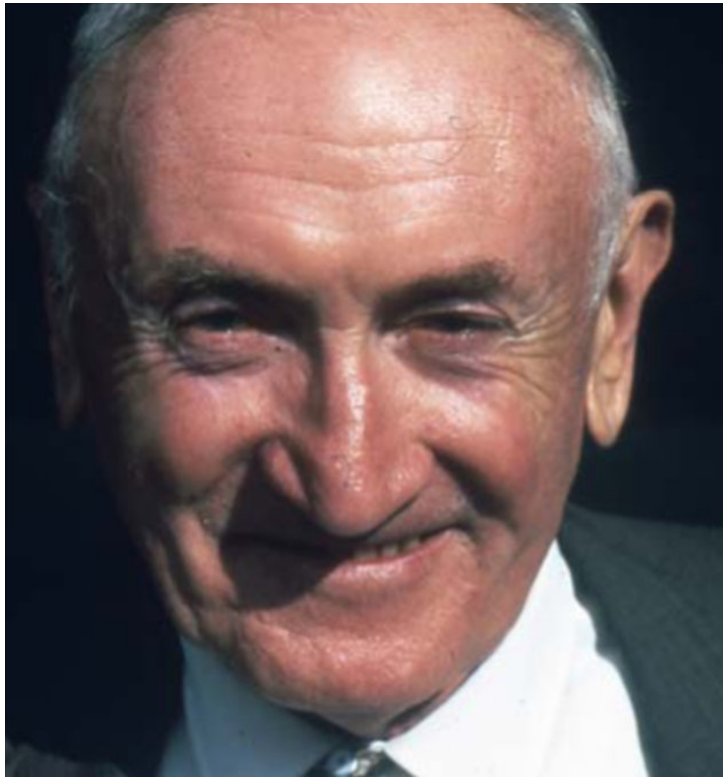

Fritz Zwicky
1898 - 1974

- **Tired light** is a class of hypothetical redshift mechanisms that was proposed as an alternative explanation for the redshift-distance relationship.
- The concept was first proposed in 1929 by Fritz Zwicky, suggesting that photons lost energy over time through collisions with other particles in a regular way.
- Tired light has been proposed as the Steady State cosmologies.

"Tired-Light" Hypothesis Gets Re-Tired

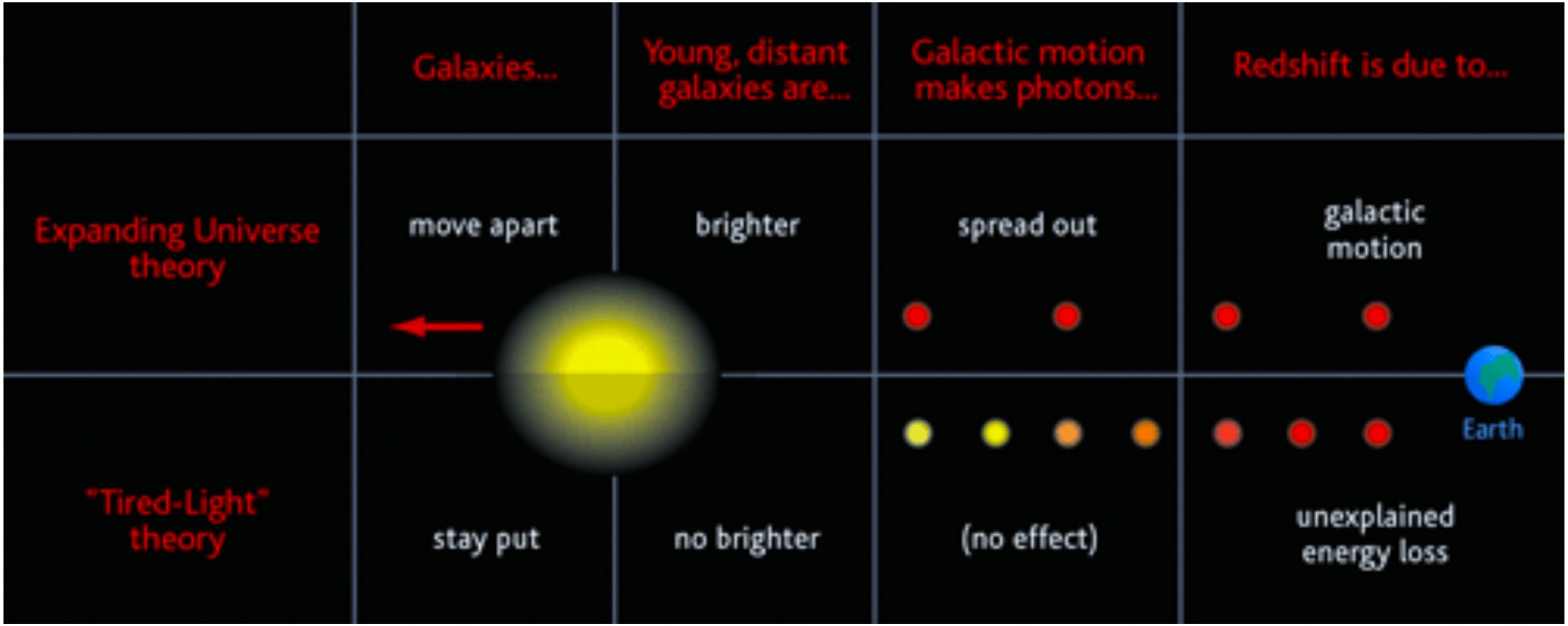

Beyond the fringe. "Tired light"--a radical alternative to the standard expanding-universe model of the cosmos--has just failed two crucial tests.

Science/News, 2001

Hubble Law

$$v = c\frac{\Delta\lambda}{\lambda} = Hr$$

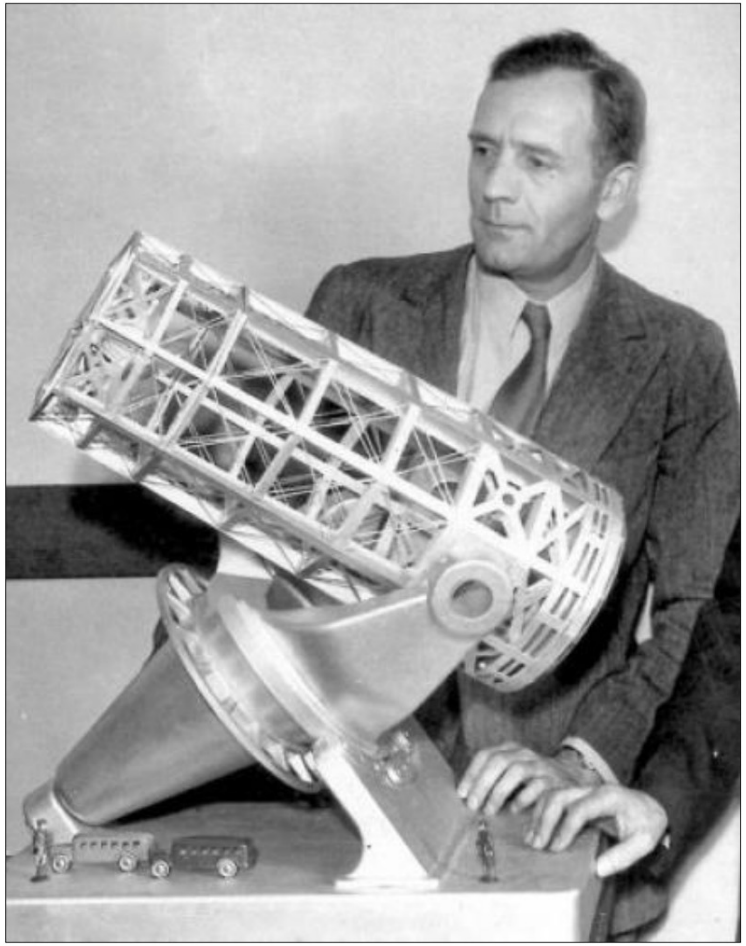

Figure 1: Edwin Hubble with a model of the proposed 200-in telescope, this is a cropped version of a photograph that appeared in the *New York Sun* on 18 June 1931 (adapted from citizensvoice.com/news/silvered-stargazer-1.1869195).

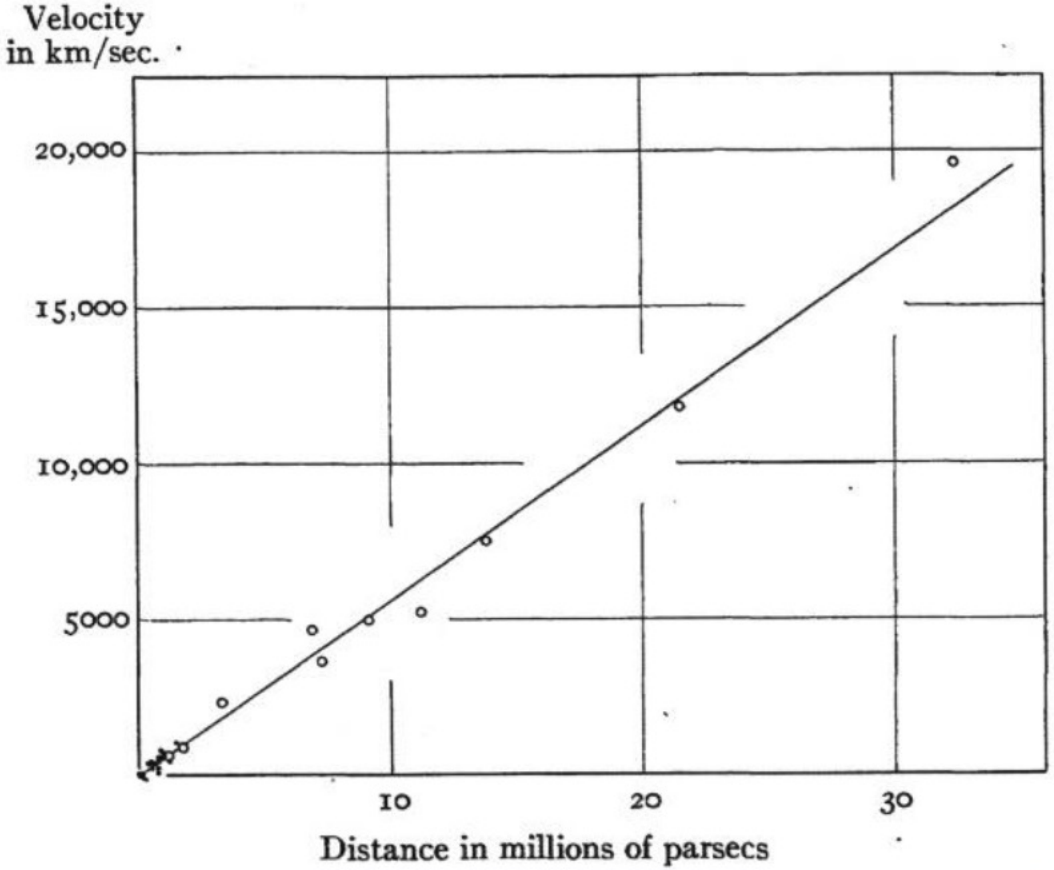

Figure 2: The Hubble law (after Hubble & Humason, 1931: 74).

Helge Kragh, ***Journal of Astronomical History and Heritage***, **20(1), 2–12 (2017).**

Possible Models of the Expanding Universe

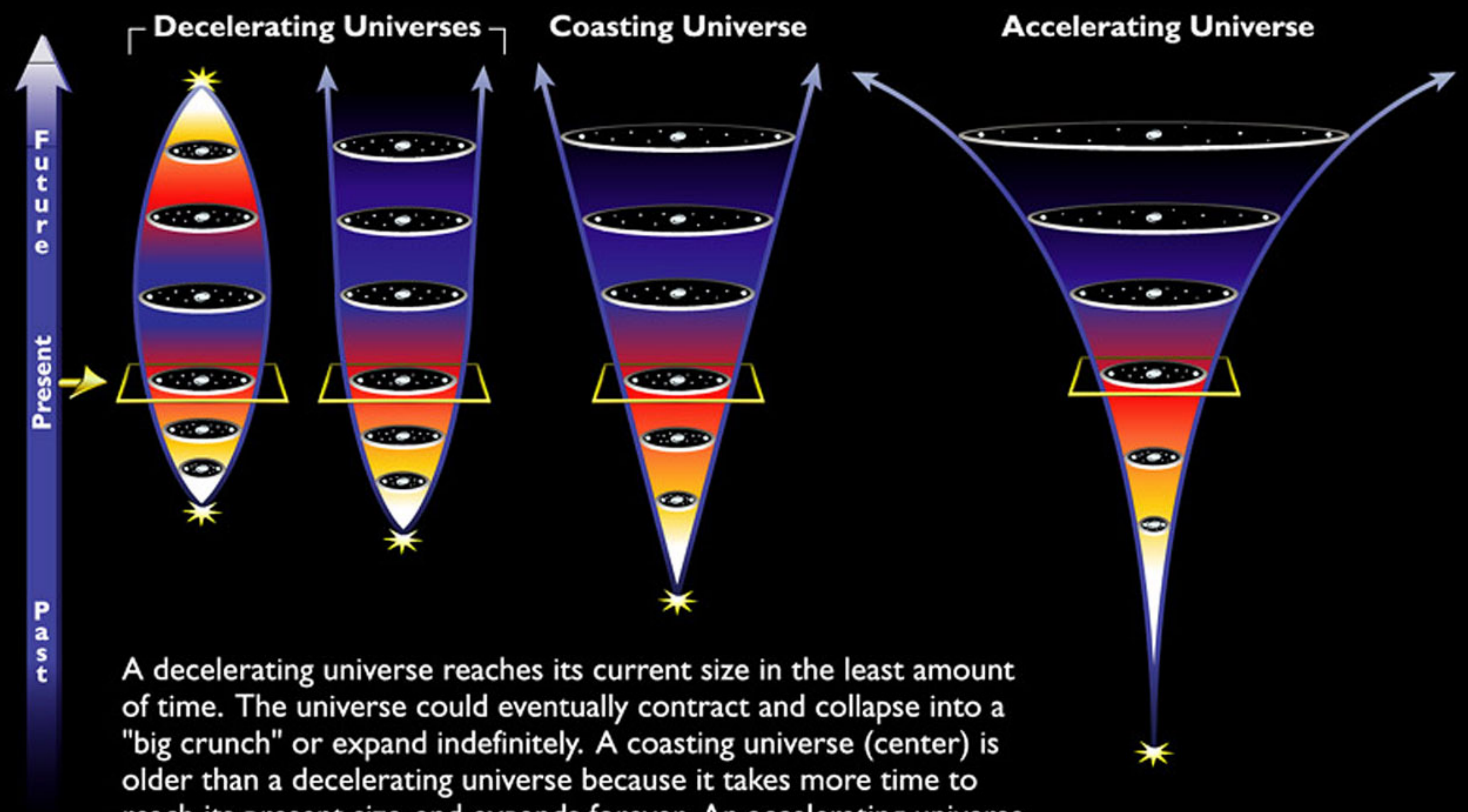

A decelerating universe reaches its current size in the least amount of time. The universe could eventually contract and collapse into a "big crunch" or expand indefinitely. A coasting universe (center) is older than a decelerating universe because it takes more time to reach its present size, and expands forever. An accelerating universe (right) is older still. The rate of expansion actually increases because of a repulsive force that pushes galaxies apart.

PUBLICATIONS OF THE ASTRONOMICAL SOCIETY OF THE PACIFIC, **112**:1284–1299, 2000 October

Invited Review

The Case for an Accelerating Universe from Supernovae

ADAM G. RIESS[1,2]

Received 2000 May 4; accepted 2000 May 5

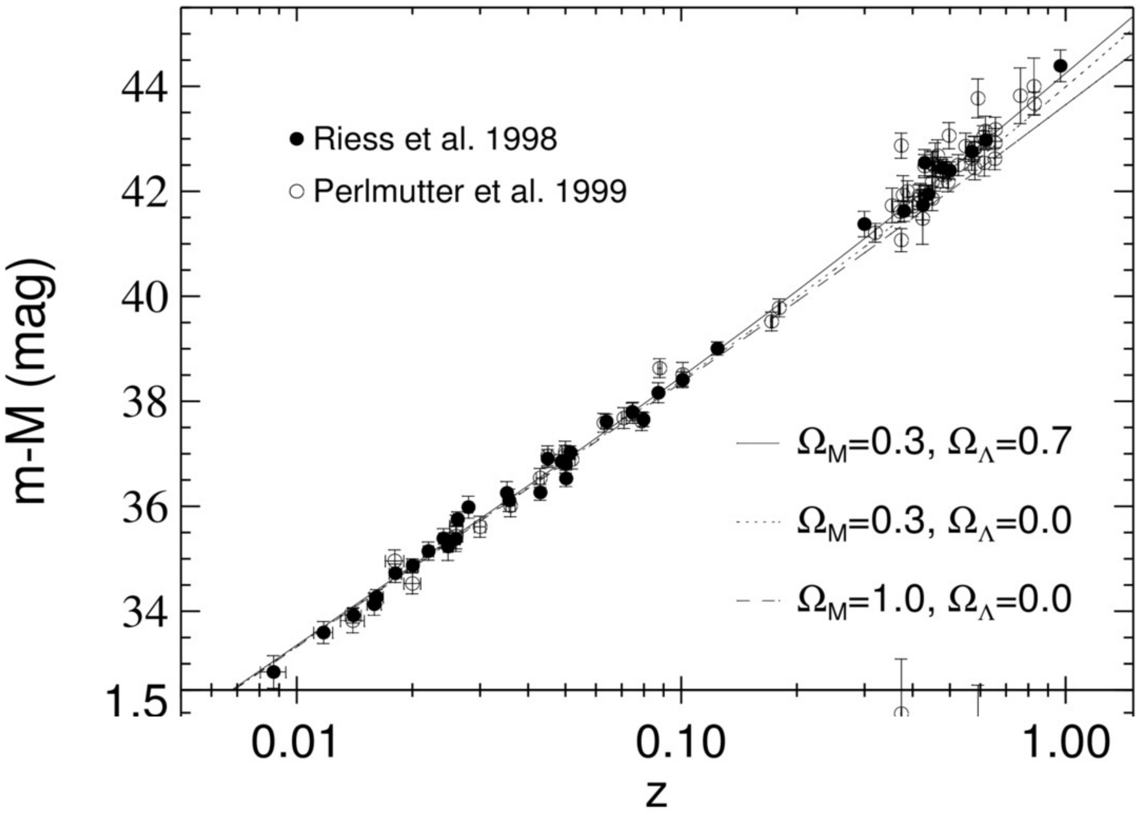

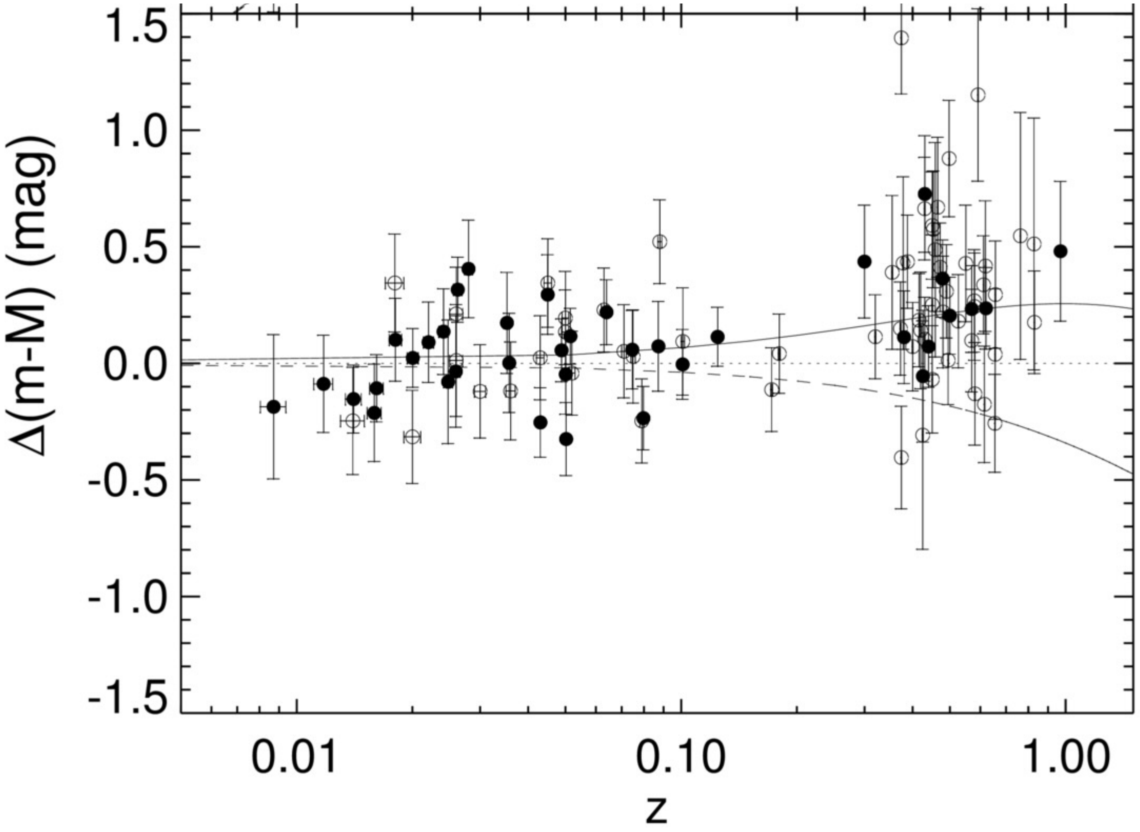

The Big Bang

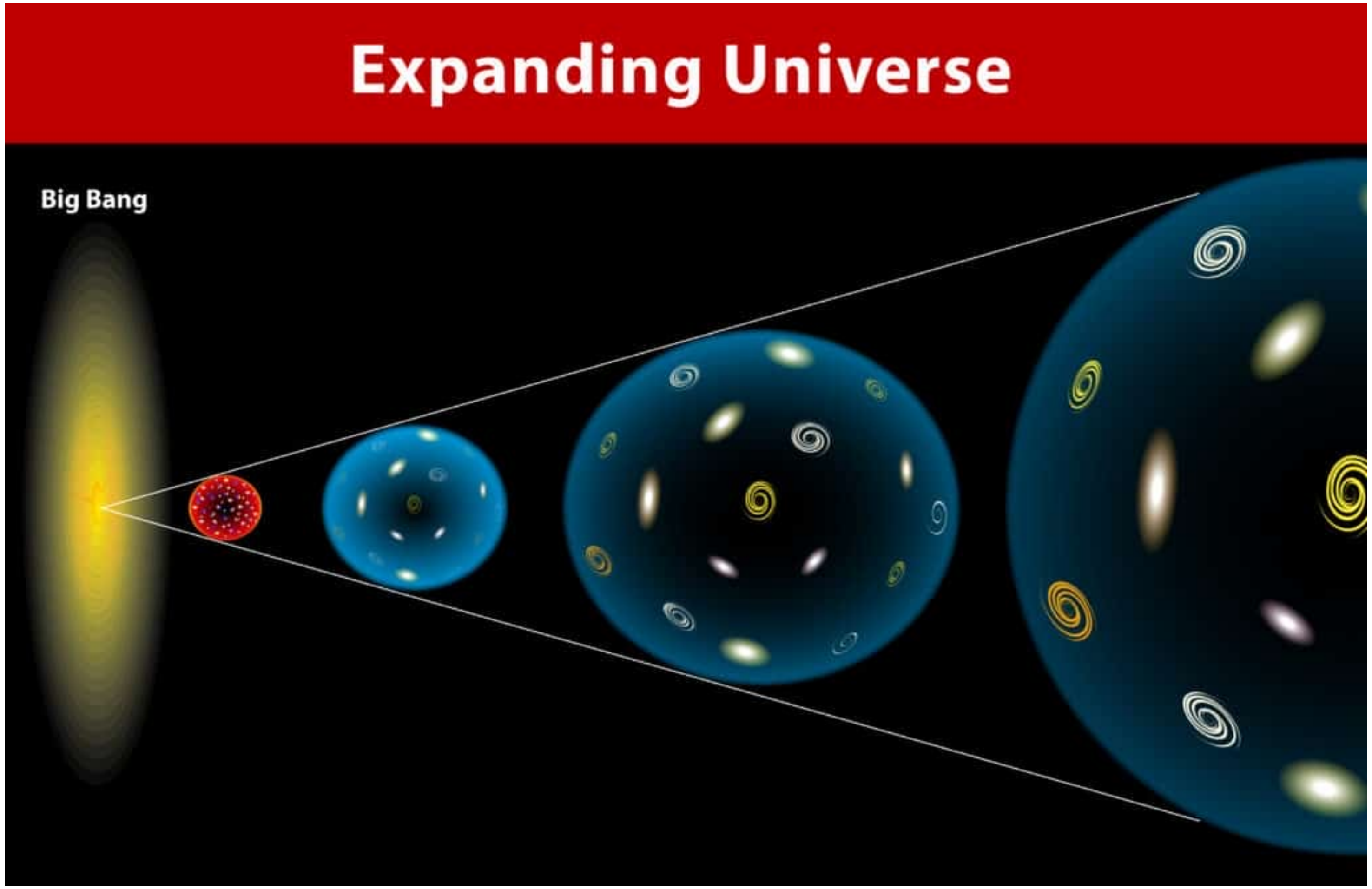

https://www.science-sparks.com/

Implication of Big Bang Theory:

Cosmic Microwave Background (CMB)

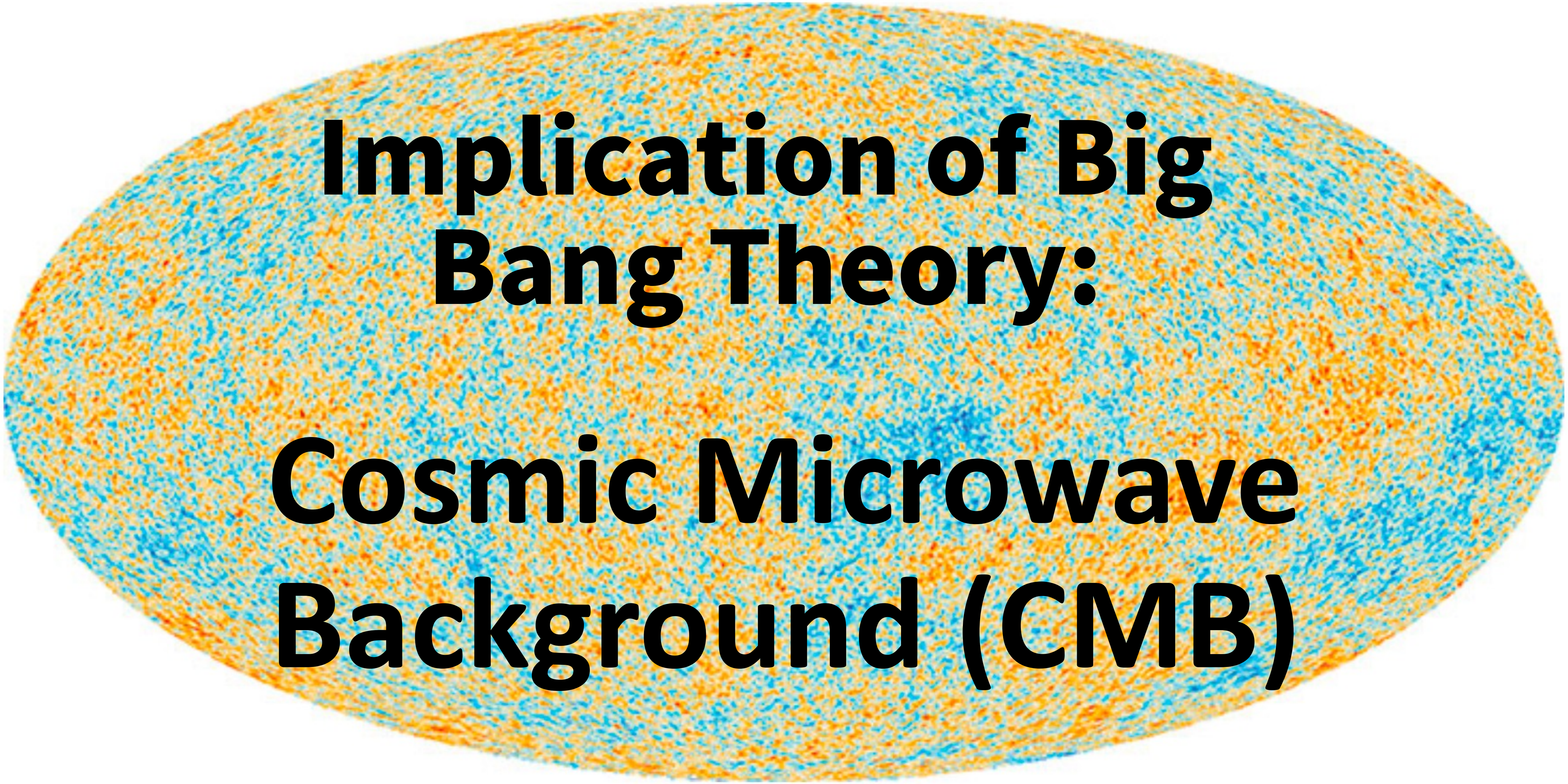

Cosmic Microwave Background

In 1964, Arno Penzias and Robert Wilson at Bell Telephone Laboratories made their first measurement clearly showing the presence of the microwave background

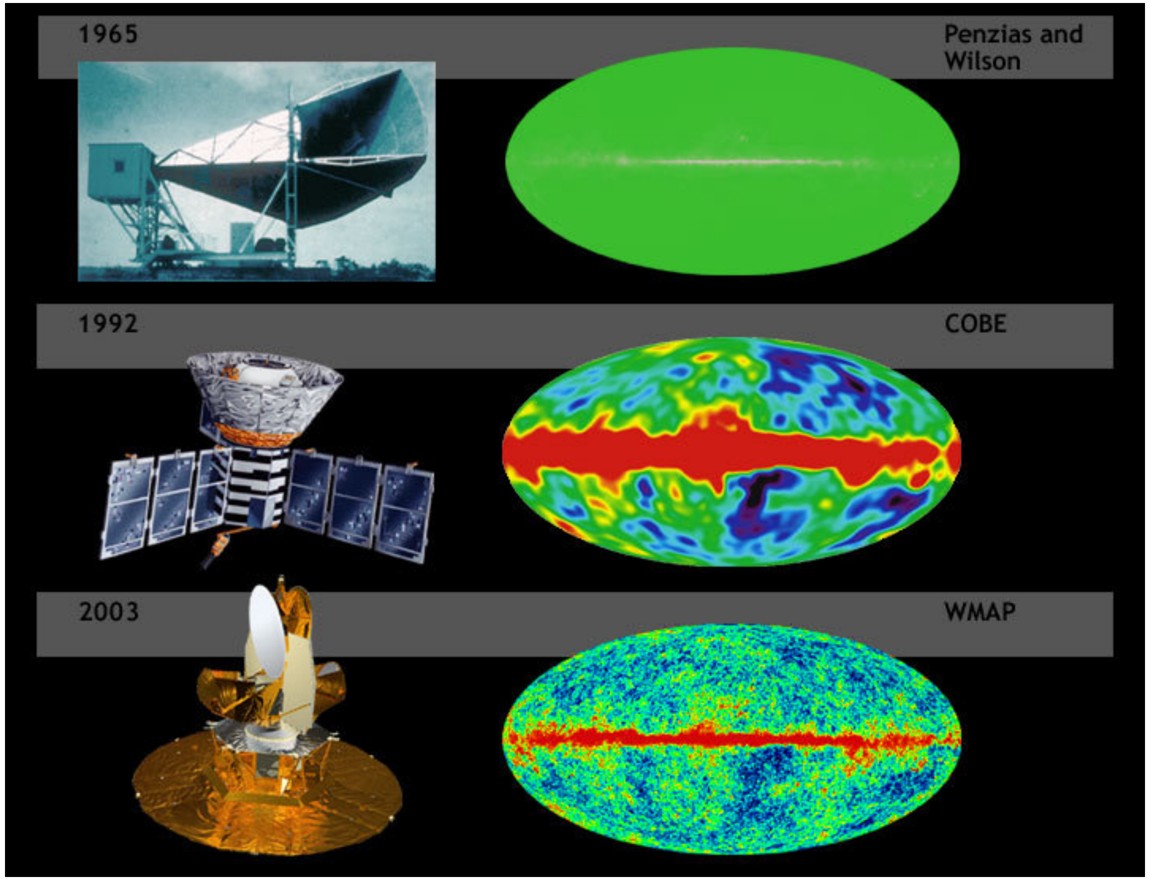

Cosmic Microwave Background

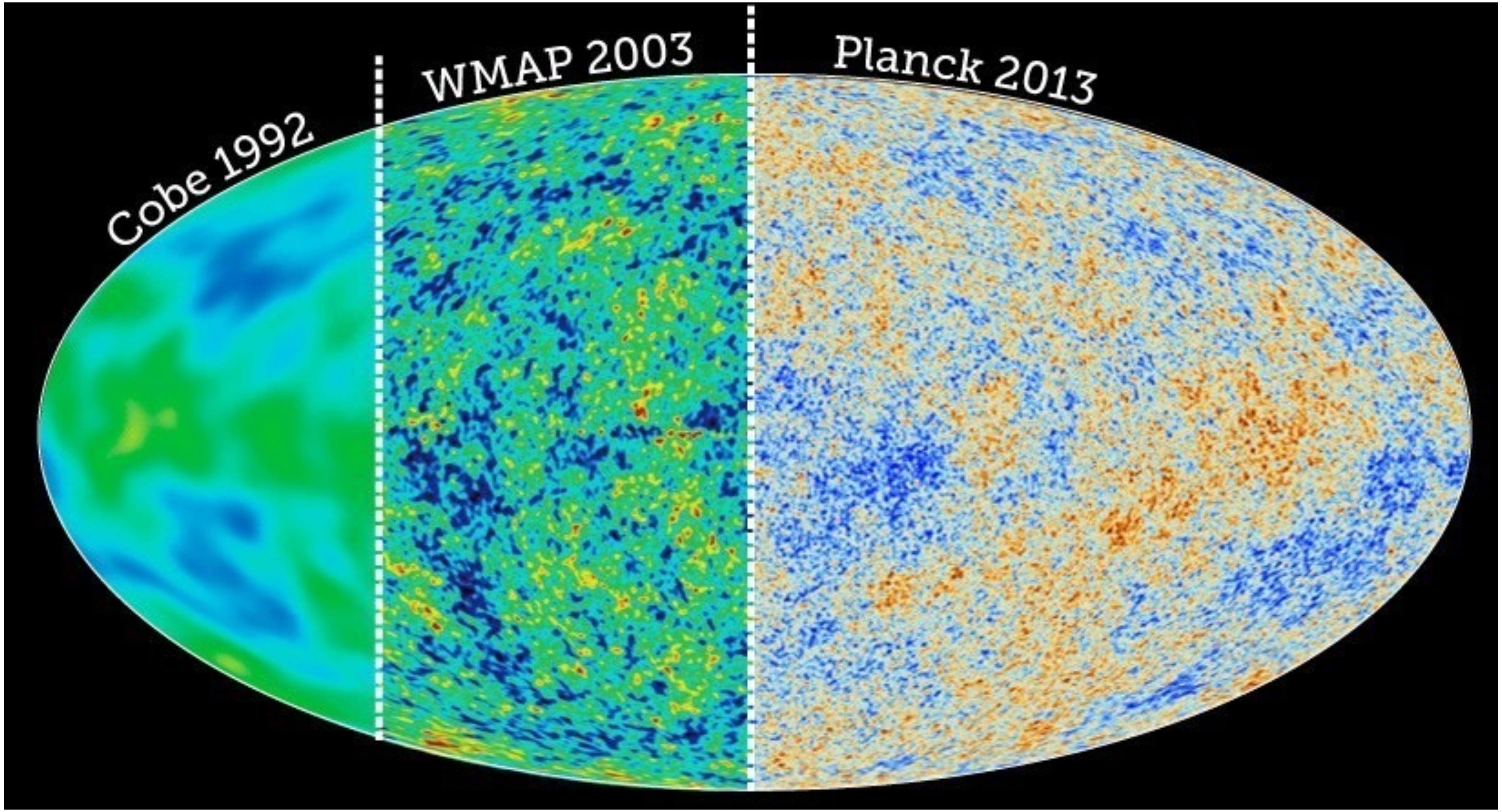

CMB – PLANK

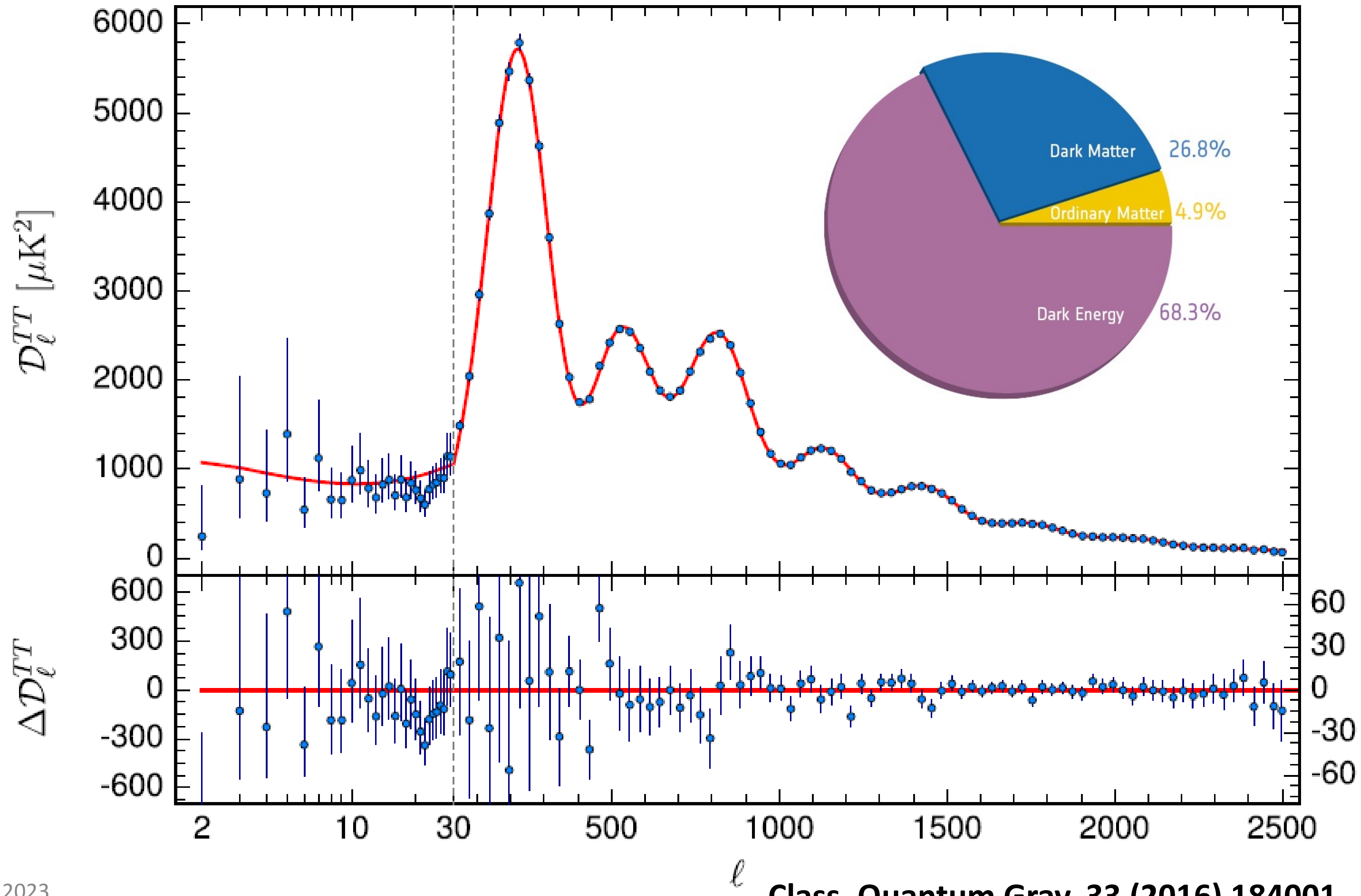

Class. Quantum Grav. 33 (2016) 184001

Standard Cosmology

- Expanding universe
- ΛCDM - accelerating universe with cold dark matter (CDM)
- Bottom-up structure formation
- Galaxies, galaxy clusters, larger cosmic structures
- Challenges

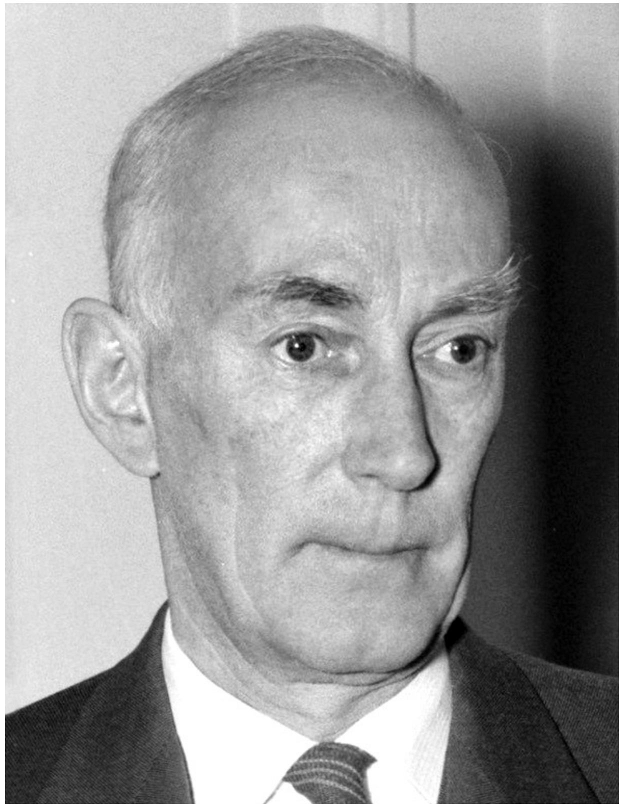

Jan Oort

1900 - 1902

In 1932, Oort found that the mass obtained from the dynamics was three times greater than that of the luminous matter in Milky Way. Oort introduced the concept of "dark matter" for the first time.

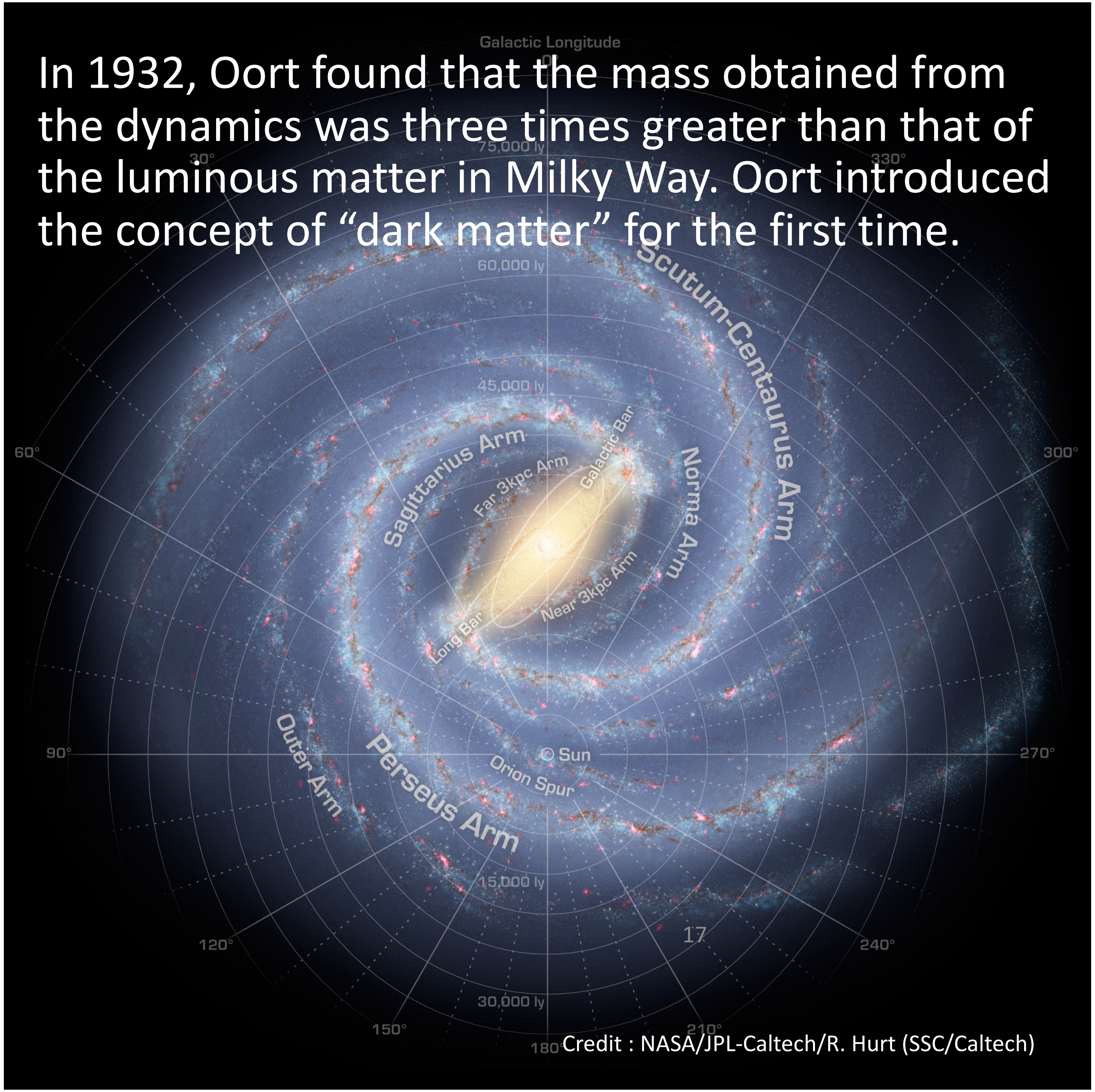

Credit : NASA/JPL-Caltech/R. Hurt (SSC/Caltech)

Computer Simulation

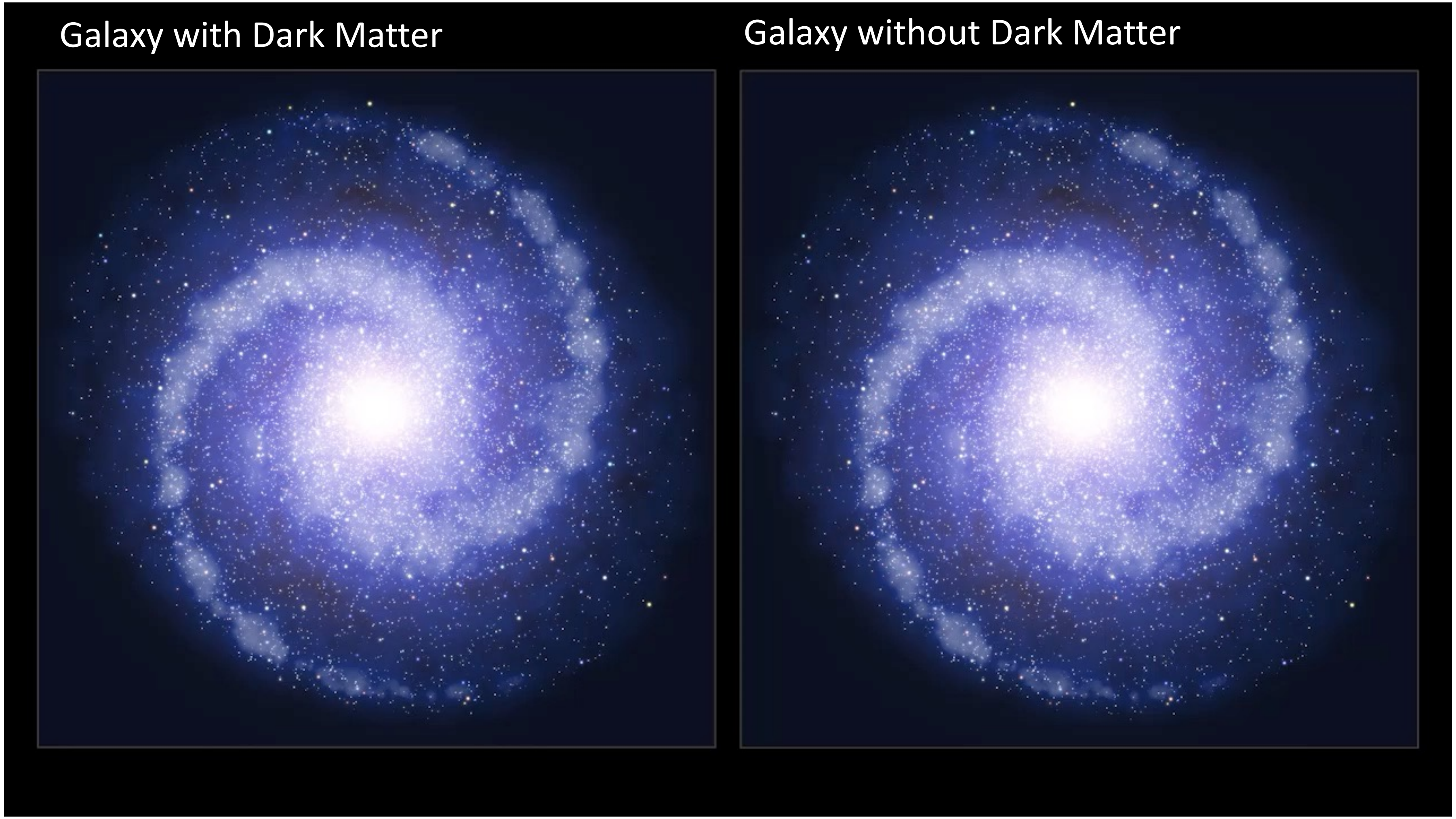

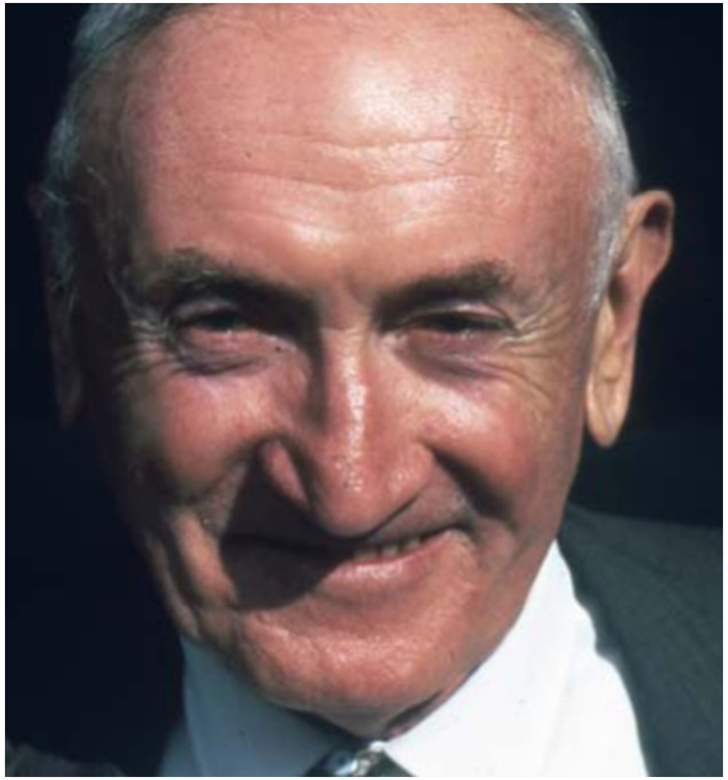

Fritz Zwicky
1898 - 1974

In 1933, Zwicky discovered that the galaxies on the outskirts of the Coma Cluster were moving too fast, and the gravitational pull provided by the luminous matter was not sufficient to bind these galaxies.

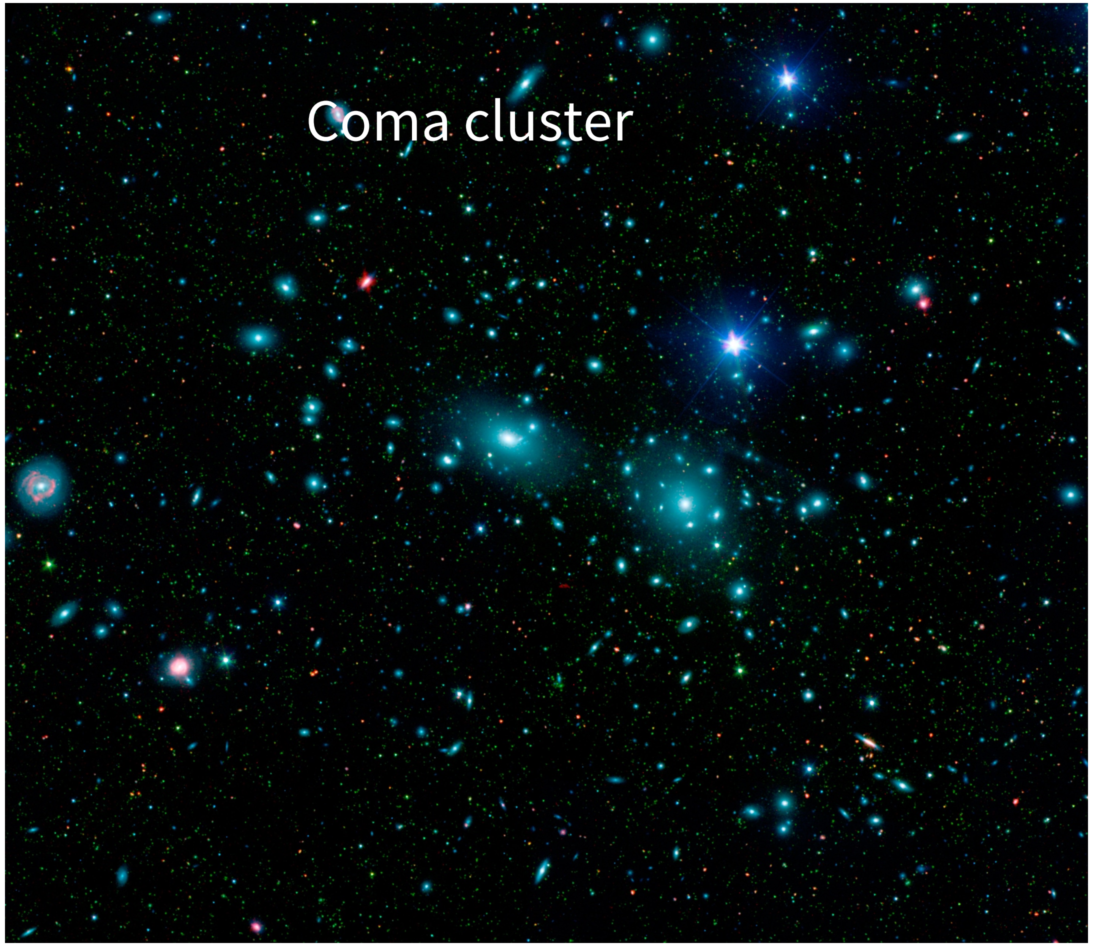

Flat Rotation Curve

Vera Rubin

Albert Bosma

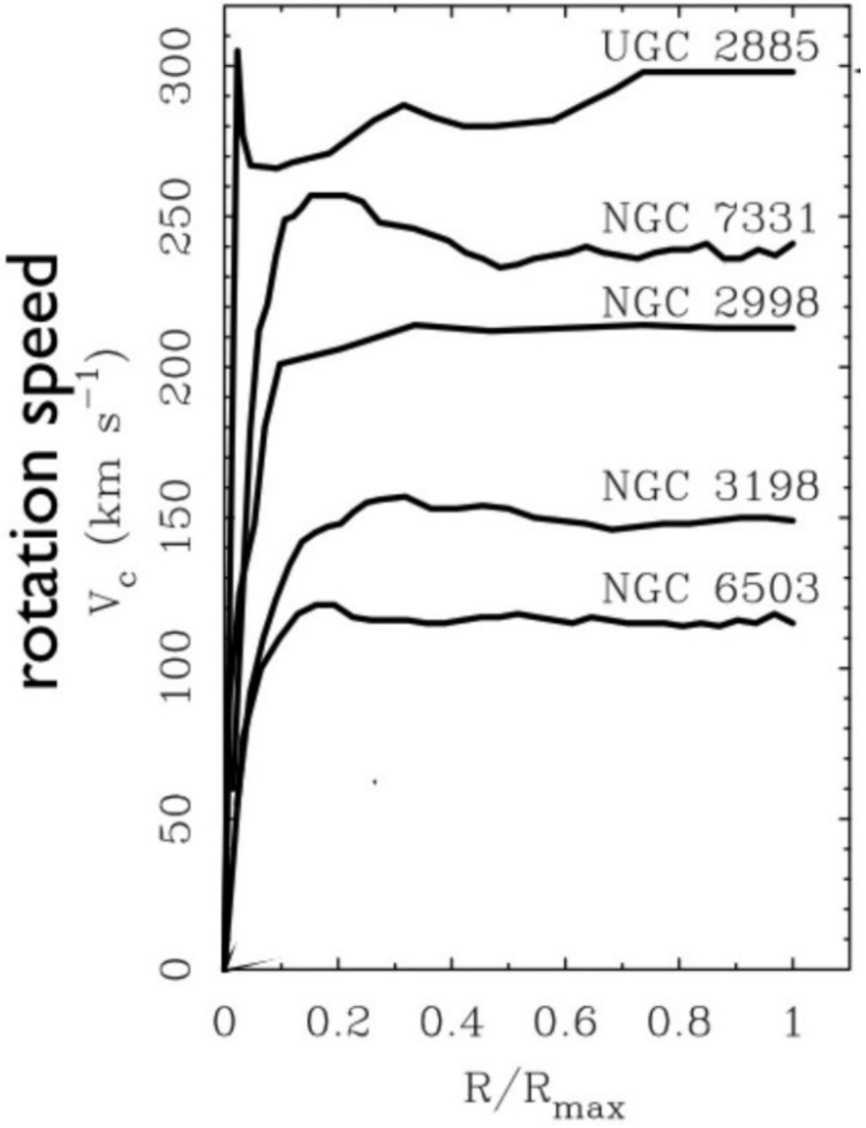

$$a = g$$

$$\rightarrow \frac{v^2}{r} = \frac{GM}{r^2}$$

$$\rightarrow v \propto \frac{1}{\sqrt{r}}$$

“Dark Matter” (DM)

- A hypothetical form of matter invisible to electromagnetic radiation, postulated to account for gravitational forces observed in the universe.
- Dark Matter Span 90 Orders of Magnitude in Mass.

- None has been directly detected!

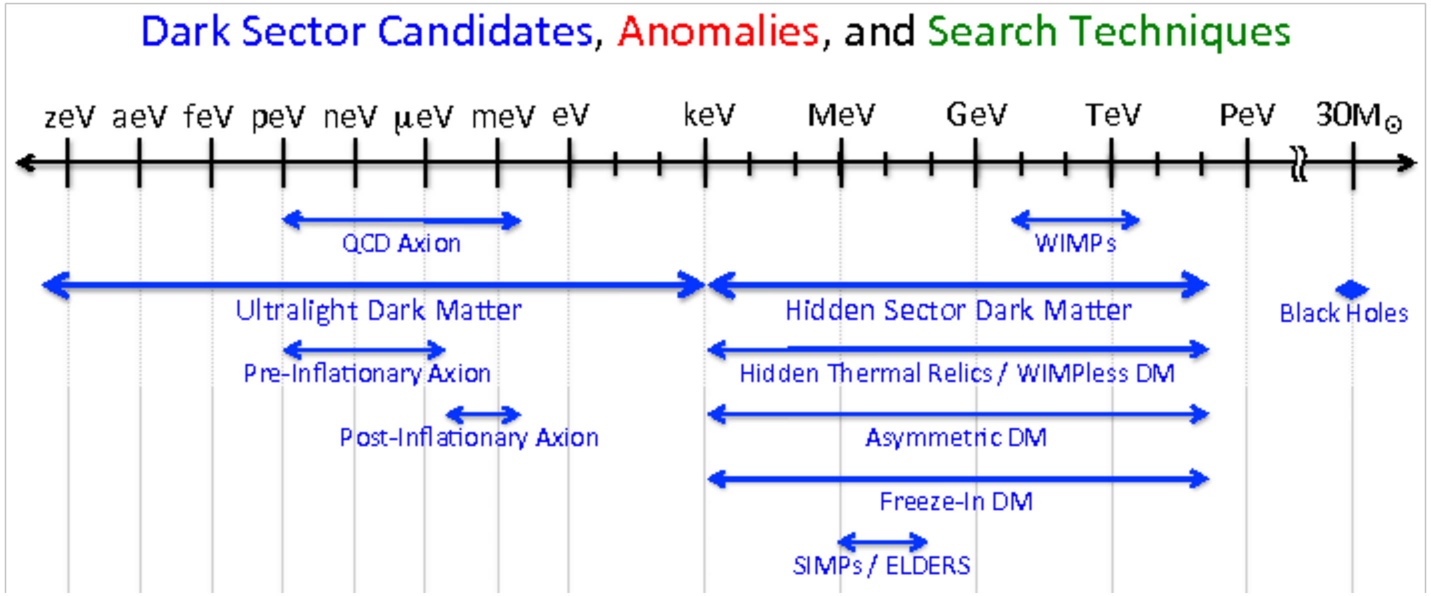

Beyond standard model in particle physics

Modified Newtonian Dynamics (MOND)

Mordehai Milgrom
Israeli Physicist
1946 -

Proposed by Milgrom in 1983

$$\boldsymbol{\mu}\left(\left|\frac{\mathbf{g}_{obs}}{a_0}\right|\right)\mathbf{g}_{obs} = \mathbf{g}_{bar}$$

i. as $g_{obs} \gg a_0$, $\mu\left(\left|\frac{g_{obs}}{a_0}\right|\right) \approx 1$

ii. as $g_{obs} \ll a_0$, $\mu\left(\left|\frac{g_{obs}}{a_0}\right|\right) \approx \left|\frac{g_{obs}}{a_0}\right|$

where $\boldsymbol{a_0 = 1.2 \times 10^{-10} ms^{-2}}$

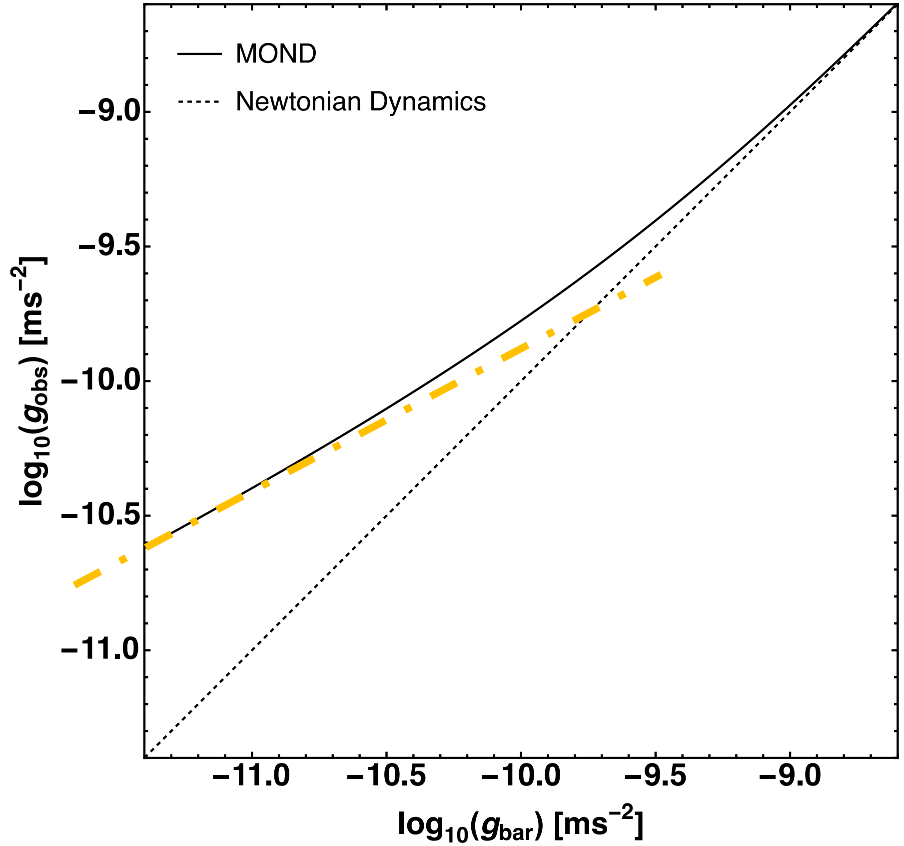

Beyond Newtonian Dynamics and General Relativity

more idea…

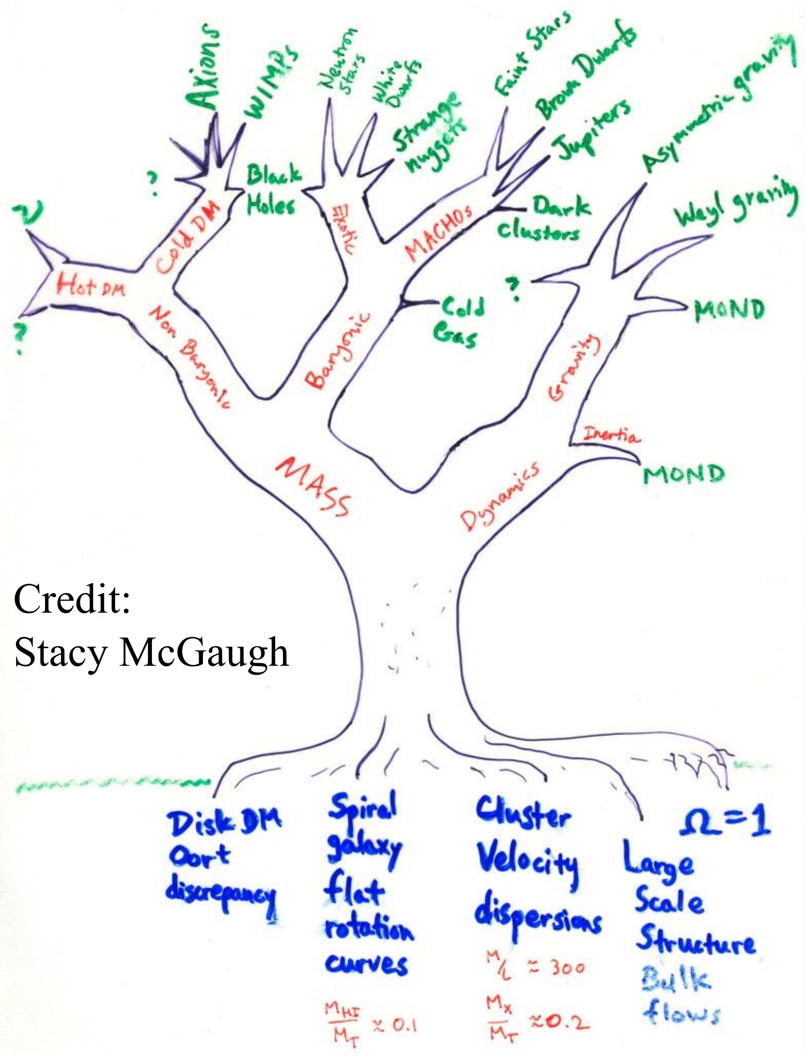

Credit:
Stacy McGaugh

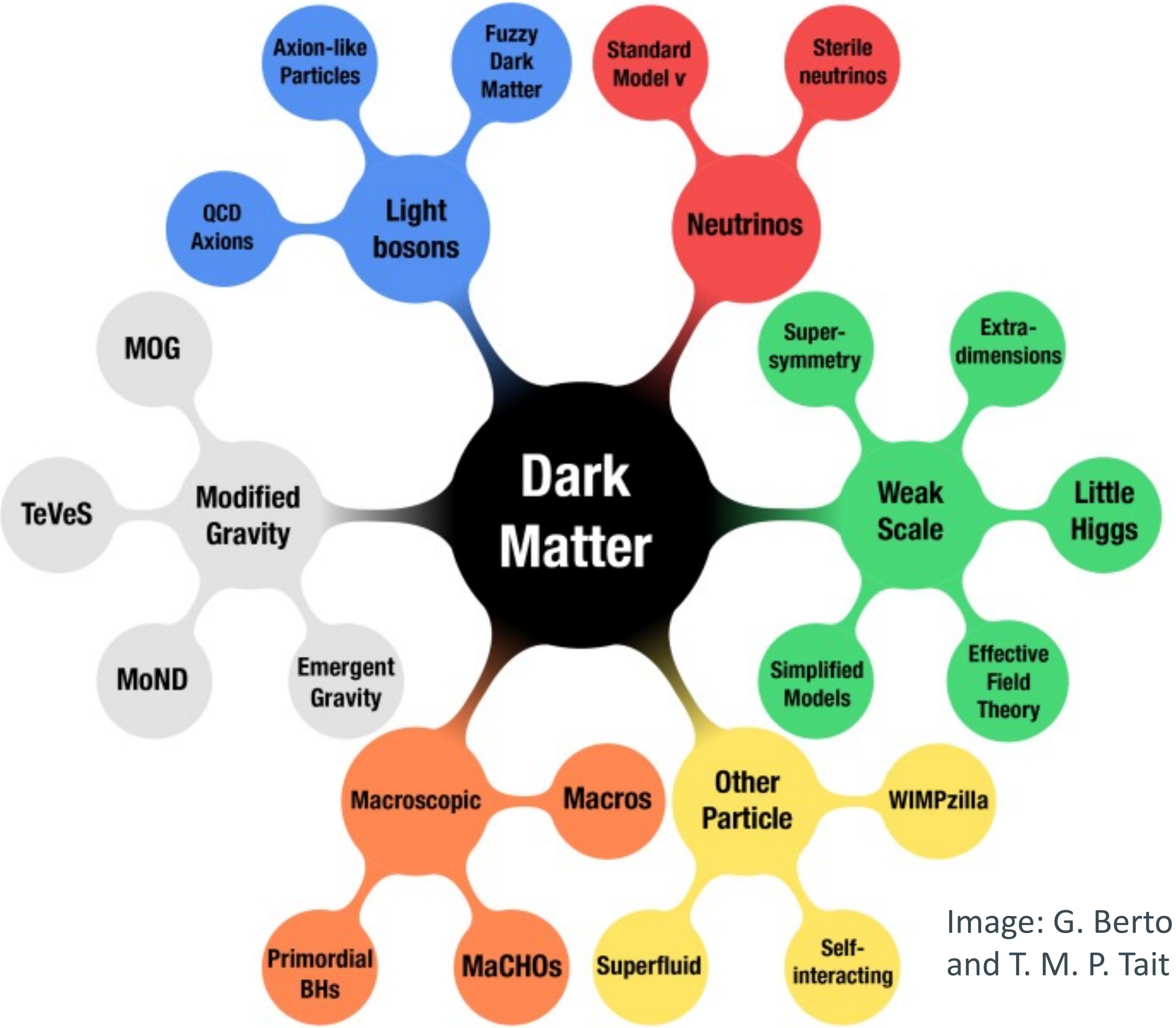

Image: G. Bertone and T. M. P. Tait

“Missing Mass Problem”

❖ Definitions of two accelerations:

Newton’s law — **Newton’s gravity**

$$\boldsymbol{g_{obs} \equiv |-\nabla\Phi_{obs}|} \quad =? \quad \boldsymbol{g_{bar} \equiv \frac{GM_{bar}(<r)}{r^2}}$$

❖ Asumming $g_{obs} = g_{bar}$, mass discrepnacy is expected.
“dark matter” is introduced to resolve the insufficient baryonic mass.

❖ **What if $g_{obs} \neq g_{bar}$? Acceleration discrepancy instead.**

Selected for a Viewpoint in *Physics*
PRL **117,** 201101 (2016) PHYSICAL REVIEW LETTERS week ending 11 NOVEMBER 2016

Radial Acceleration Relation in Rotationally Supported Galaxies

Stacy S. McGaugh and Federico Lelli
Department of Astronomy, Case Western Reserve University, 10900 Euclid Avenue, Cleveland, Ohio 44106, USA

James M. Schombert
Department of Physics, University of Oregon, Eugene, Oregon 97403, USA
(Received 18 May 2016; revised manuscript received 7 July 2016; published 9 November 2016)

Independent measurements for two-axis:

- ❑ Vertical axis (g_{obs})

$$g_{obs} = \frac{V^2}{r}$$

- ❑ Horizontal axis (g_{bar})

$$g_{bar} = \frac{GM_{bar}(< r)}{r^2}$$

$$M_{bar} = M_{star} + M_{gas}$$

Radial Acceleration Relation

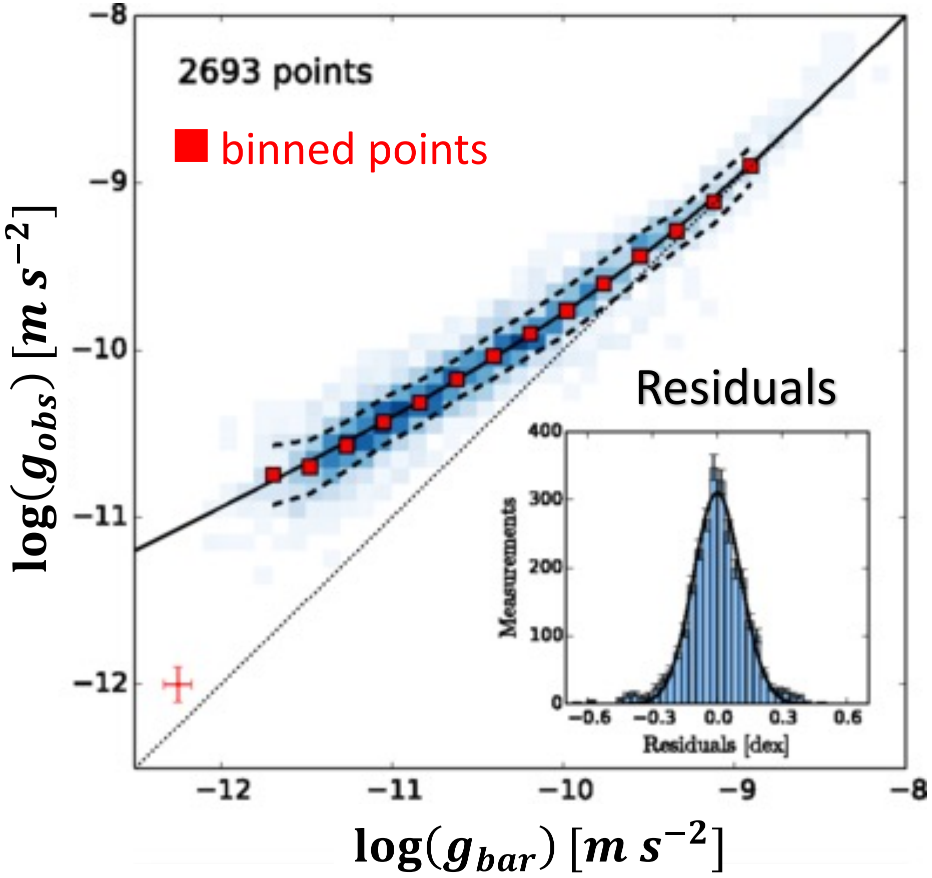

The tight relation gives

$$g_{obs} = \frac{g_{bar}}{1 - e^{-\sqrt{g_{bar}/g_\dagger}}}$$

$$g_\dagger = (1.20 \pm 0.02)\times 10^{-10}\ ms^{-2}$$

The residuals of $\log(g_{bar})$

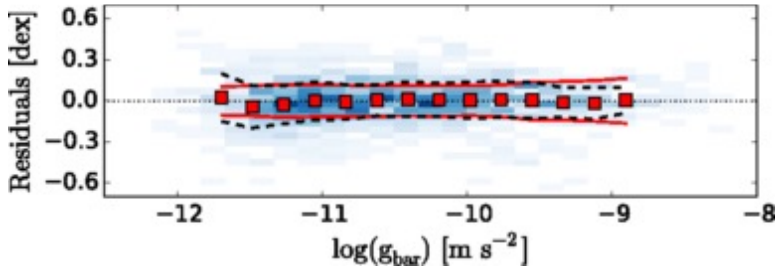

“Missing Mass” in Galaxy Cluster

Galaxy Cluster: IDCS J1426

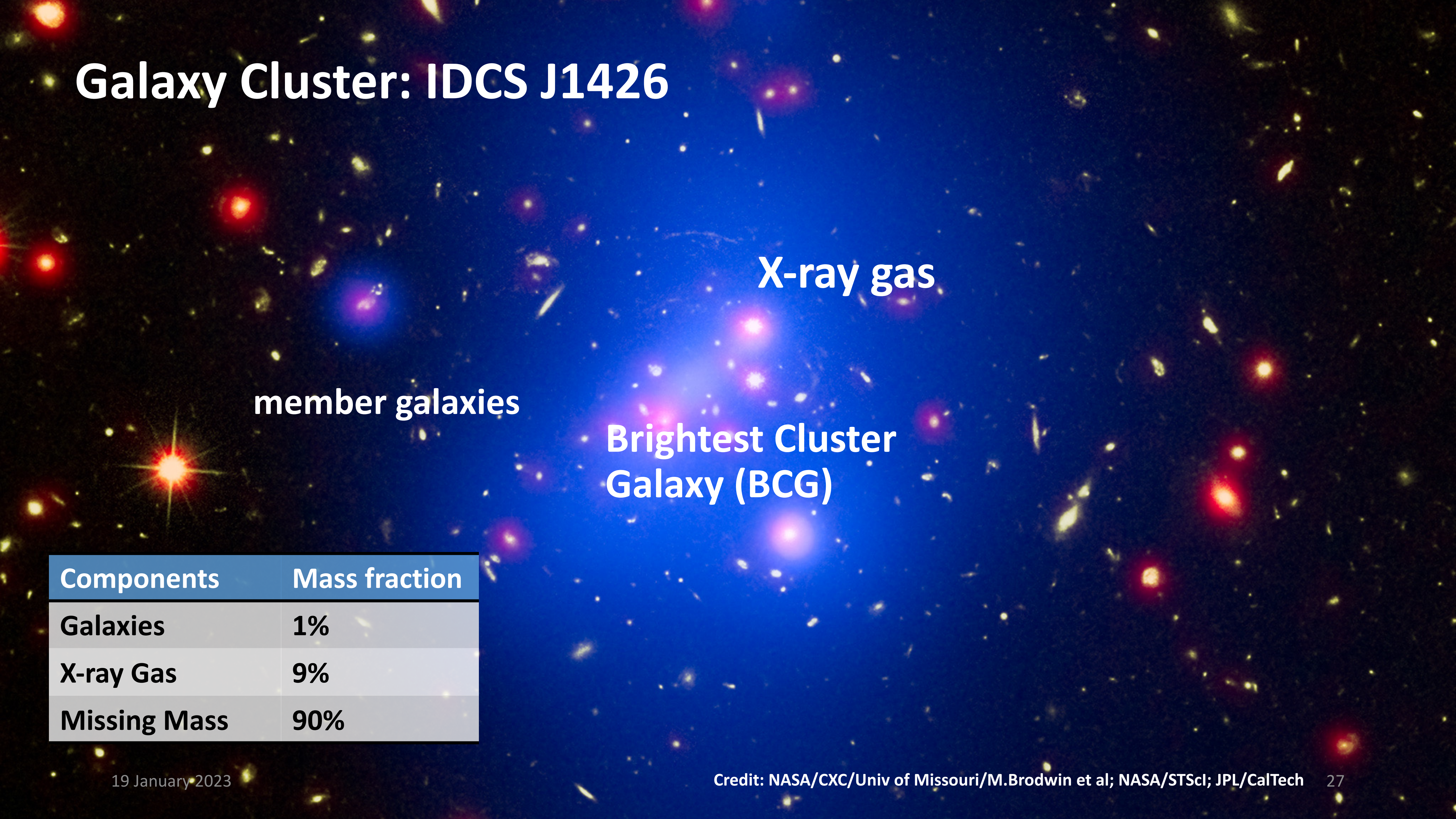

Components	Mass fraction
Galaxies	1%
X-ray Gas	9%
Missing Mass	90%

Credit: NASA/CXC/Univ of Missouri/M.Brodwin et al; NASA/STScI; JPL/CalTech

Gravitational Lensing

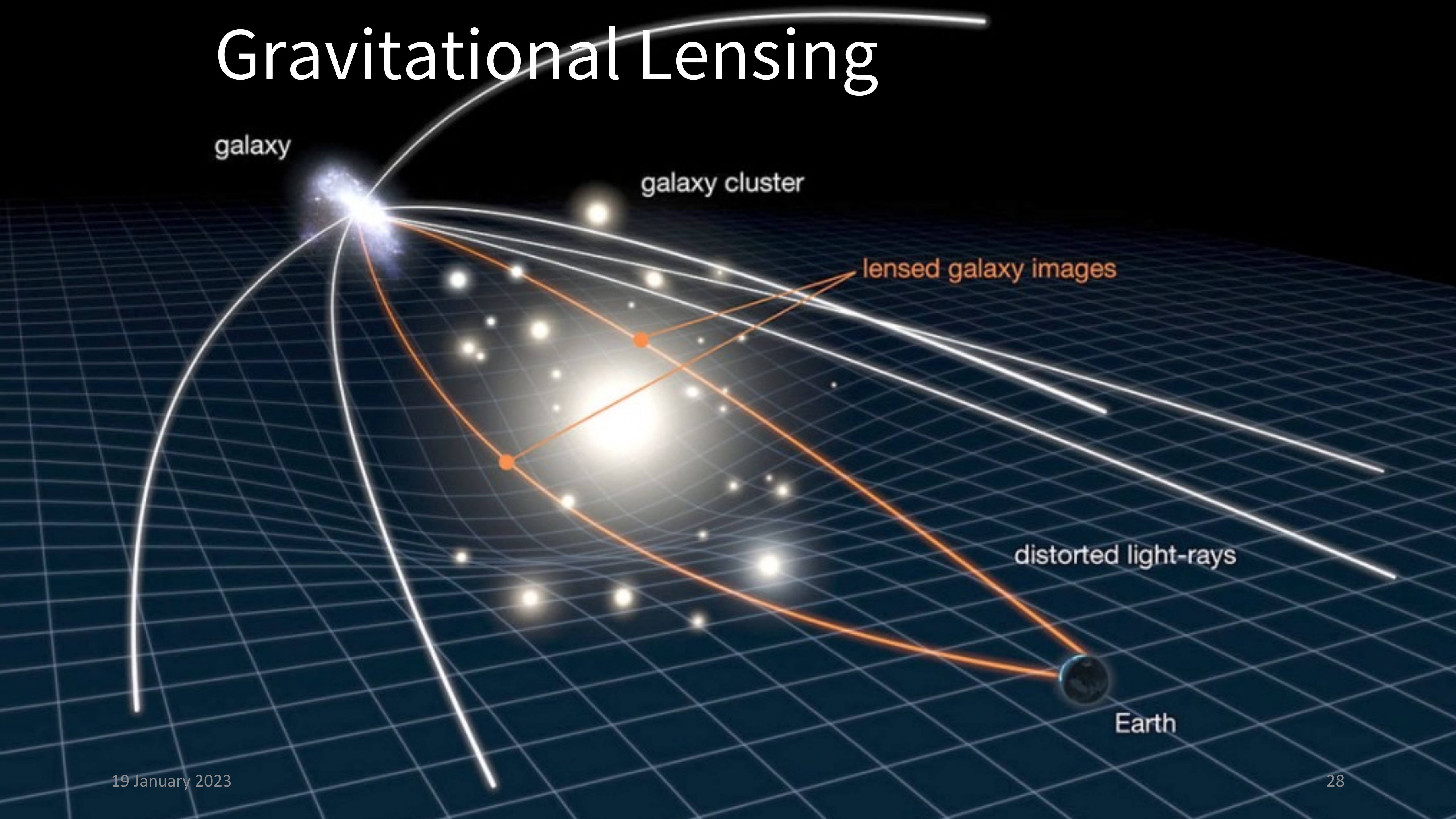

Galaxy Clusters – Weak Lensing

THE ASTROPHYSICAL JOURNAL, 821:116 (29pp), 2016 April 20 doi:10.3847/0004-637X/821/2/116

CrossMark

CLASH: JOINT ANALYSIS OF STRONG-LENSING, WEAK-LENSING SHEAR, AND MAGNIFICATION DATA FOR 20 GALAXY CLUSTERS*

KEIICHI UMETSU[1], ADI ZITRIN[2,10], DANIEL GRUEN[3,4,5,6,11], JULIAN MERTEN[7], MEGAN DONAHUE[8], AND MARC POSTMAN[9]
[1] Institute of Astronomy and Astrophysics, Academia Sinica, P. O. Box 23-141, Taipei 10617, Taiwan; keiichi@asiaa.sinica.edu.tw

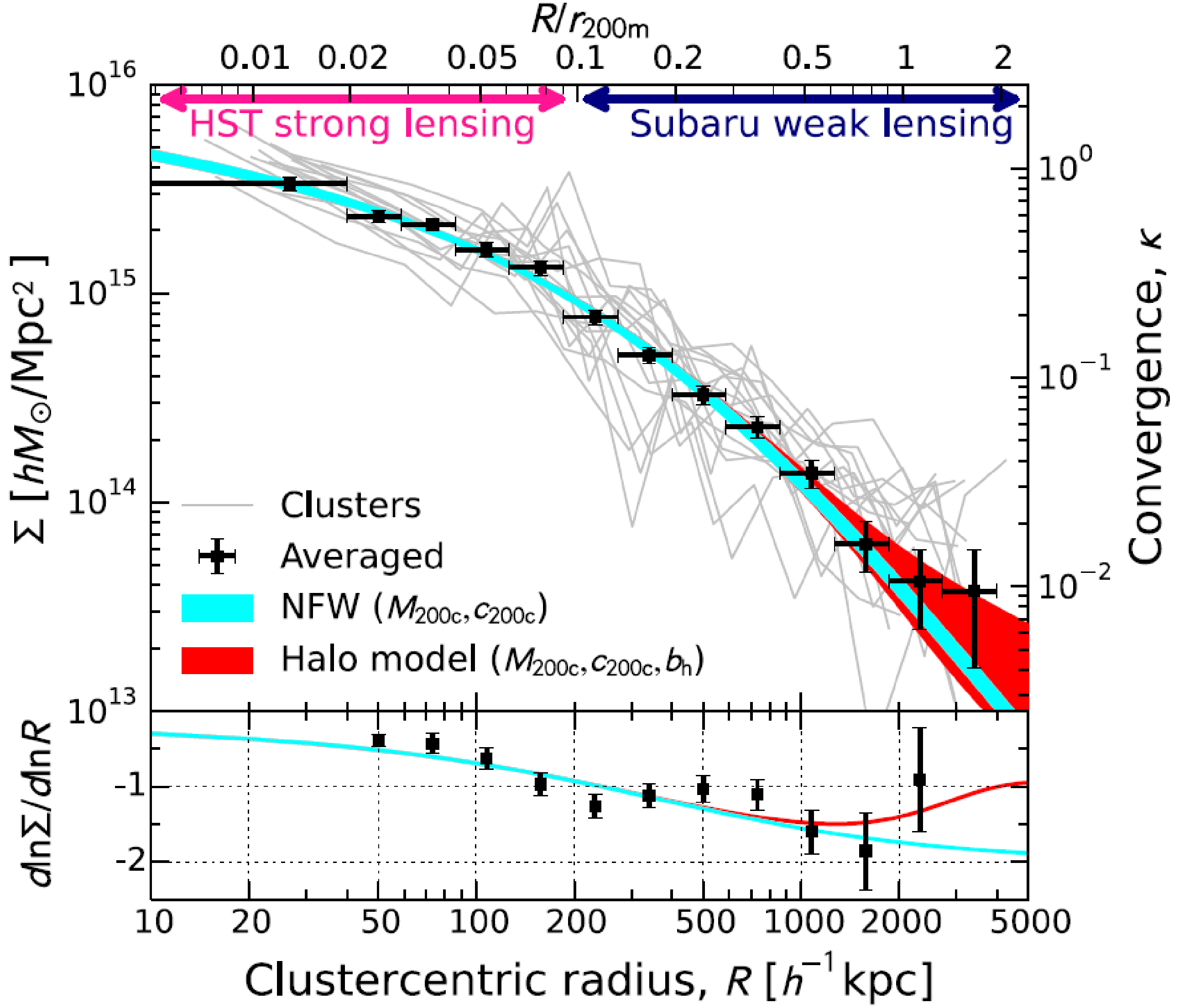

Lensing RAR on Cluster Scales?

The Astrophysical Journal, 896:70 (10pp), 2020 June 10
https://doi.org/10.3847/1538-4357/ab8e3d

The Radial Acceleration Relation in CLASH Galaxy Clusters

Yong Tian[1], Keiichi Umetsu[2], Chung-Ming Ko[1,3], Megan Donahue[4], and I-Non Chiu[2]
[1] Institute of Astronomy, National Central University, Taoyuan 32001, Taiwan; yongtian@gm.astro.ncu.edu.tw
[2] Academia Sinica Institute of Astronomy and Astrophysics (ASIAA), No. 1, Section 4, Roosevelt Road, Taipei 10617, Taiwan; keiichi@asiaa.sinica.edu.tw
[3] Department of Physics and Center for Complex Systems, National Central University, Taoyuan 32001, Taiwan; cmko@gm.astro.ncu.edu.tw
[4] Physics and Astronomy Department, Michigan State University, East Lansing, MI 48824, USA
Received 2020 January 19; revised 2020 April 23; accepted 2020 April 27; published 2020 June 15

$$g_{tot} = \sqrt{g_{bar}\, g_{\ddagger}}$$

$$g_{\ddagger} = (2.0 \pm 0.1) \times 10^{-9}\, \mathrm{ms^{-2}}$$

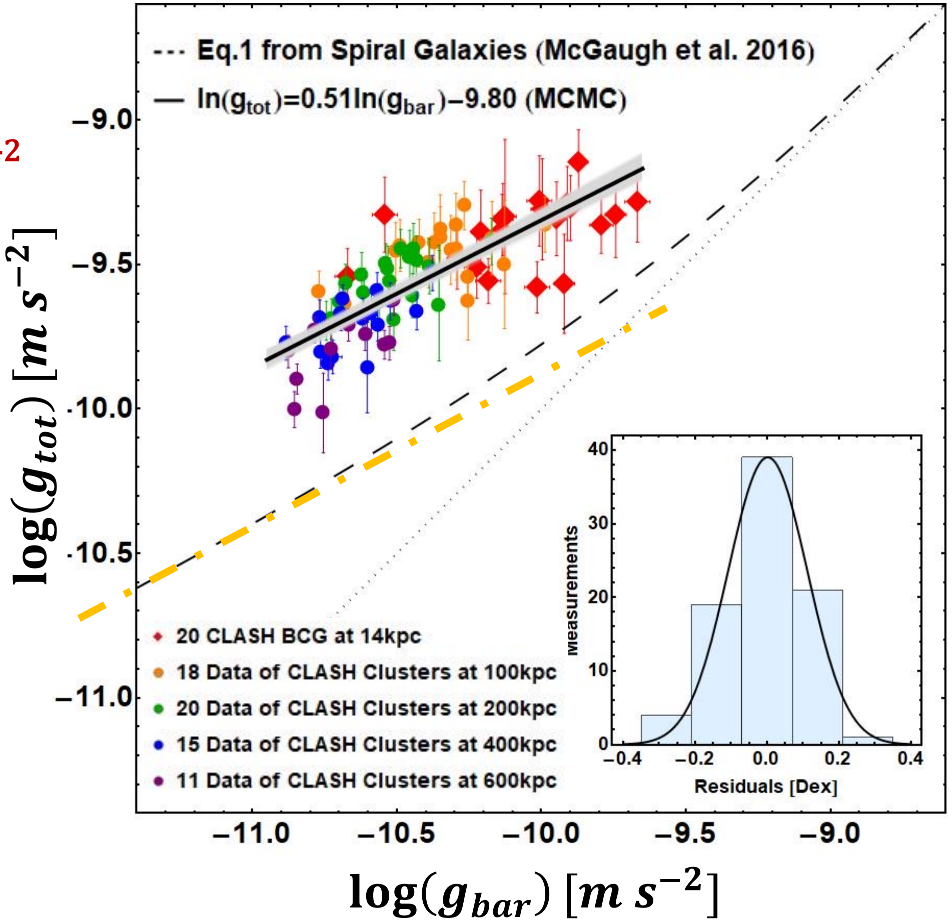

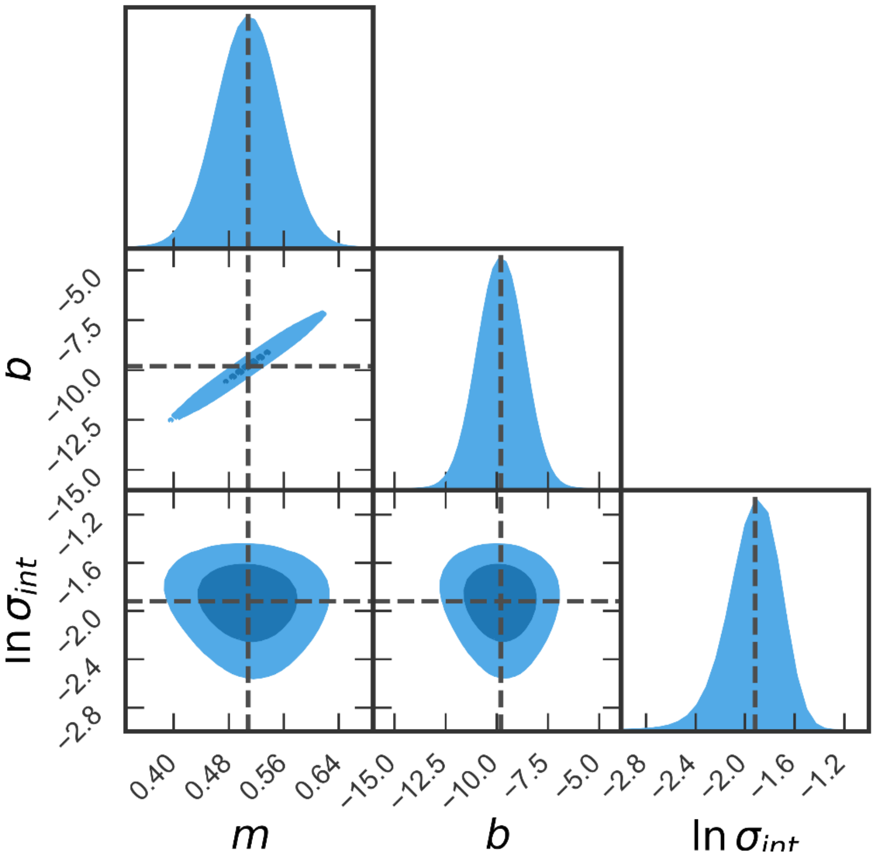

Standard Cosmology

- Expanding universe
- ΛCDM - accelerating universe with cold dark matter (CDM)
- **Bottom-up structure formation**
- Galaxies, galaxy clusters, larger cosmic structures
- Challenges

Navarro–Frenk–White (NFW) Profile

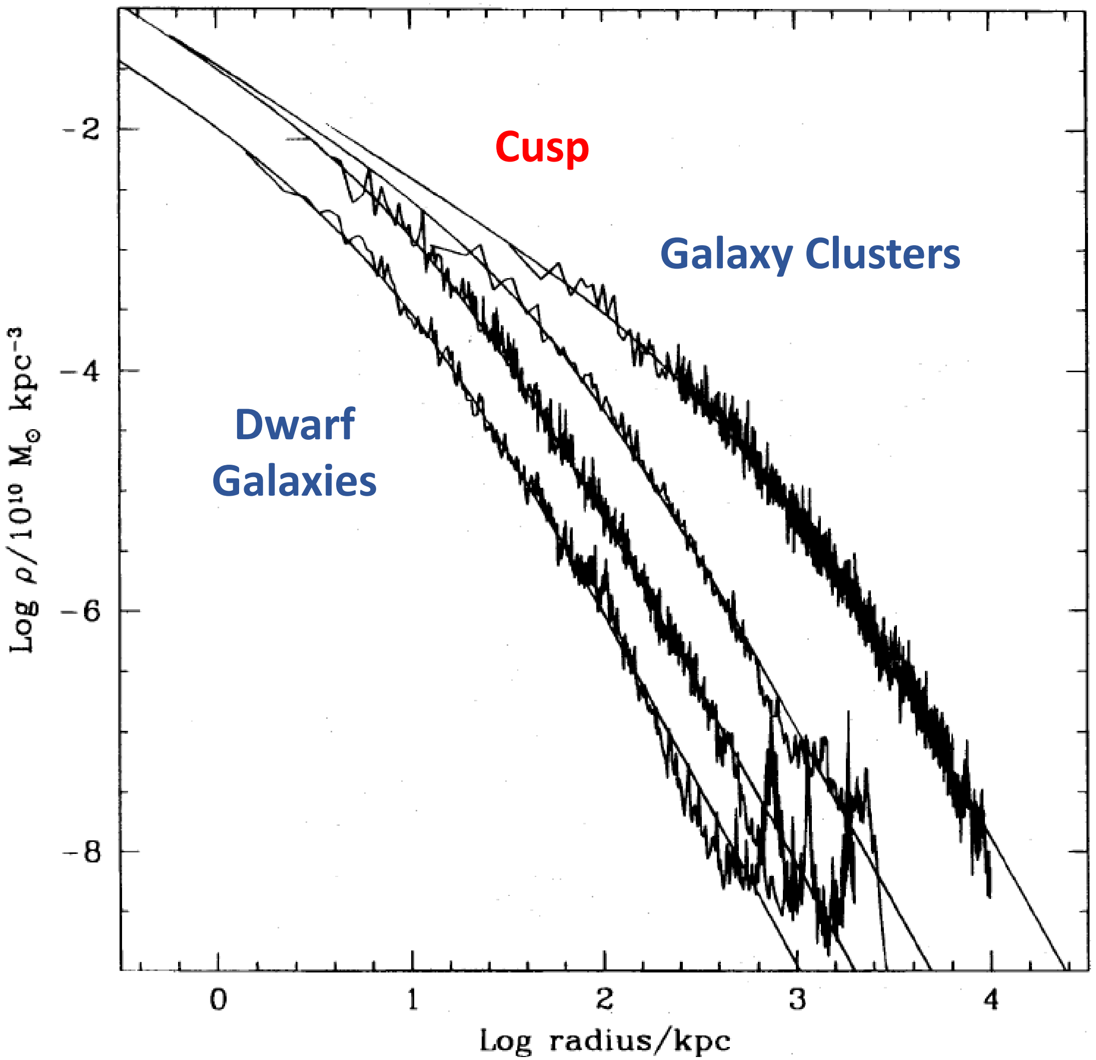

Universal density profile

$$\rho(r) = \frac{\rho_S}{\frac{r}{r_S}\left(1 + \frac{r}{r_S}\right)^2}$$

J. Navarro, C. Frenk and S. White, APJ, 462, 563 (1996)

Bottom-up Structure Formation

In a bottom-up scenario, small, dwarf galaxy-sized lumps form first, then merger to make galaxies and clusters of galaxies.

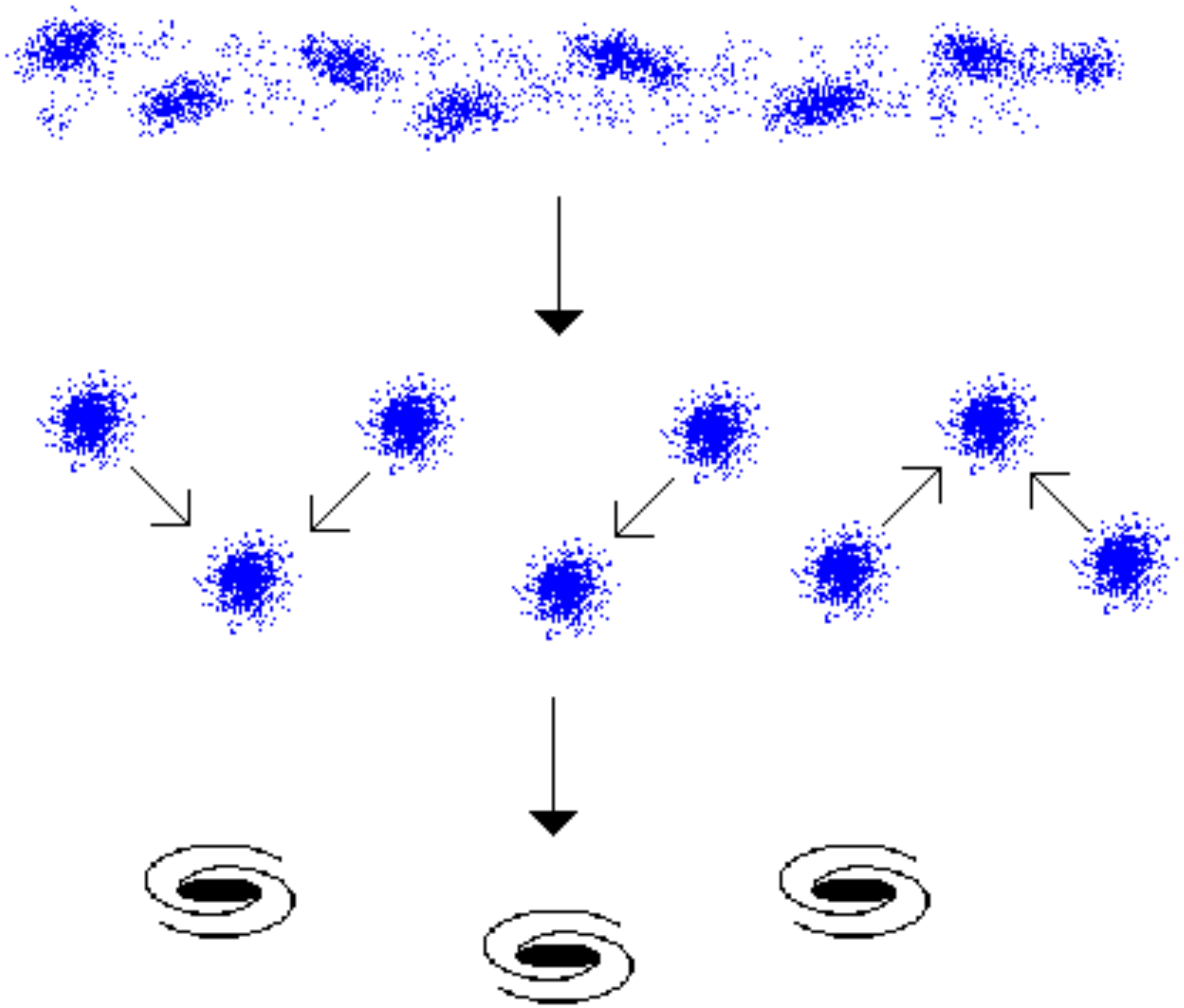

Hierarchical growth

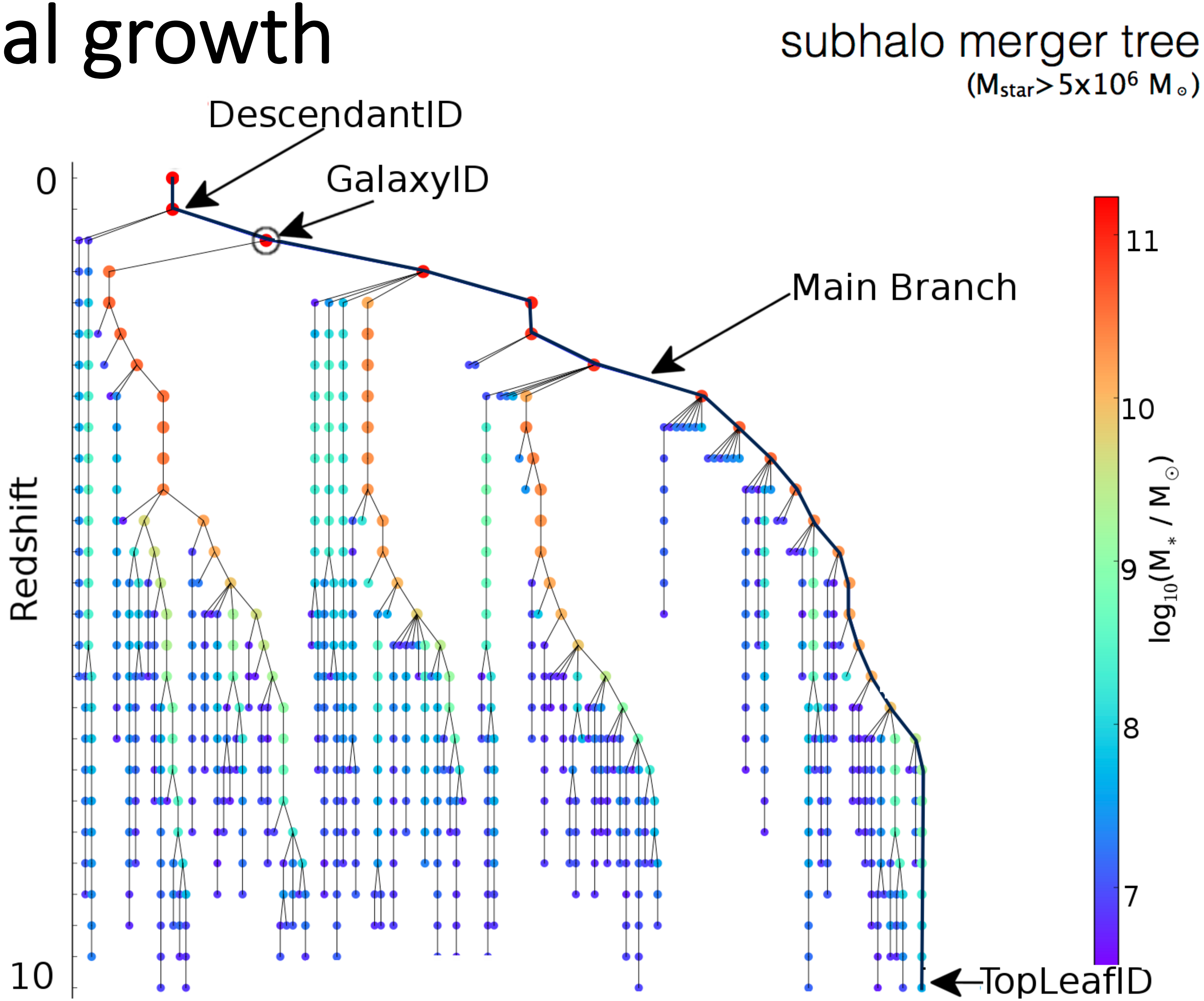

Image:
EAGLE simulation

Standard Cosmology

- Expanding universe
- ΛCDM – an accelerating universe with cold dark matter (CDM)
- Bottom-up structure formation
- **Galaxies, galaxy clusters, larger cosmic structures**
- Challenges

Galaxies

Dwarf galaxies

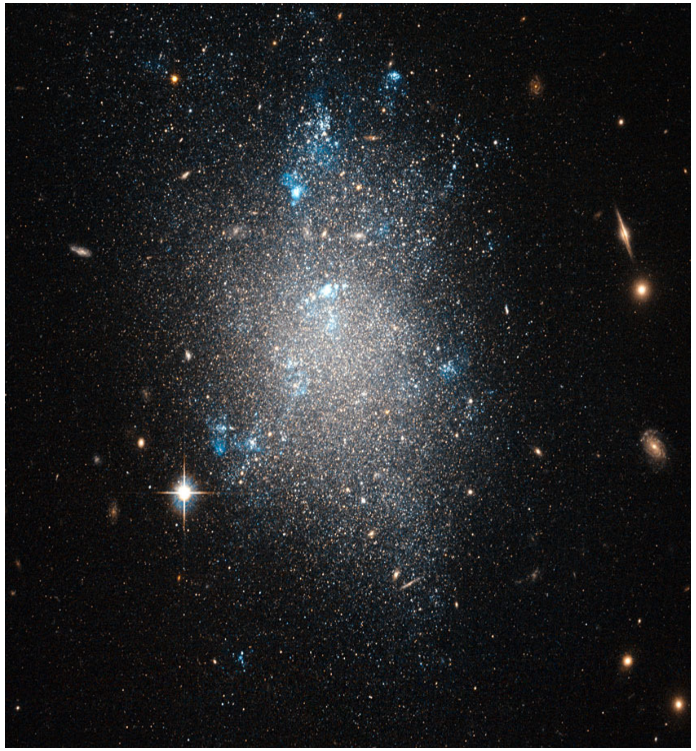

Spiral galaxies

Elliptical galaxies

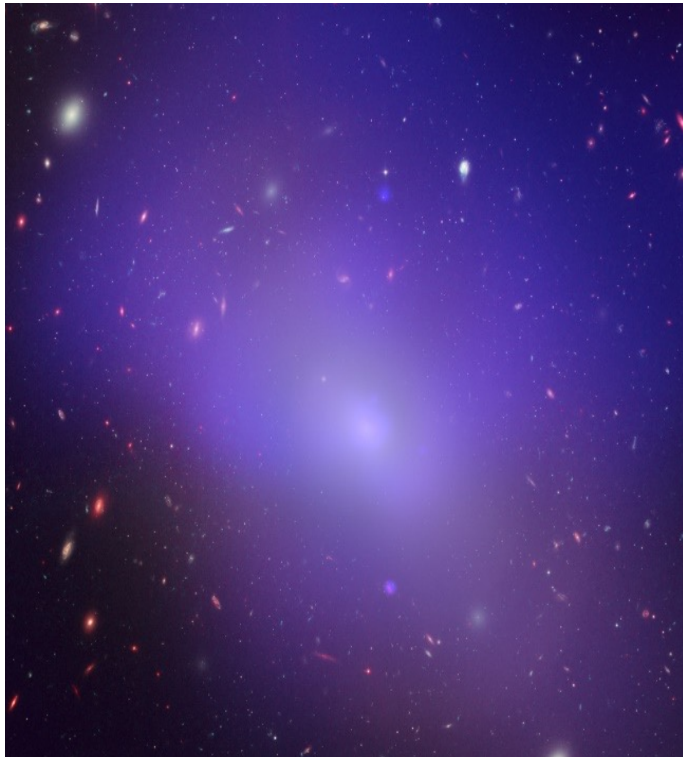

Hubble Tuning Fork

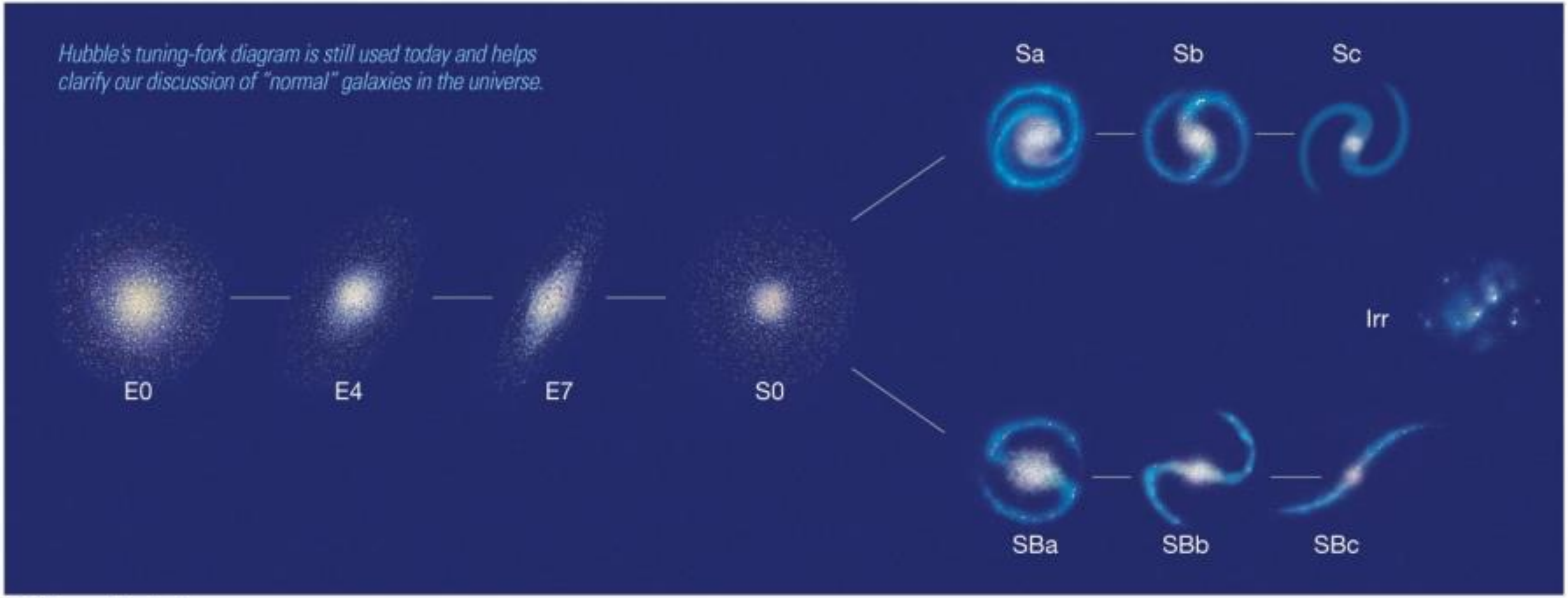

ATLAS3D

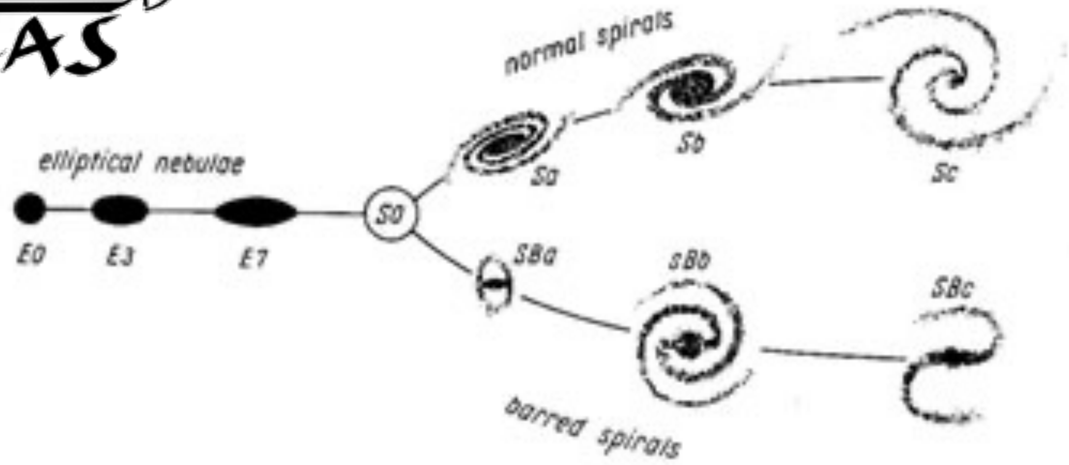

Hubble (1936) tuning fork

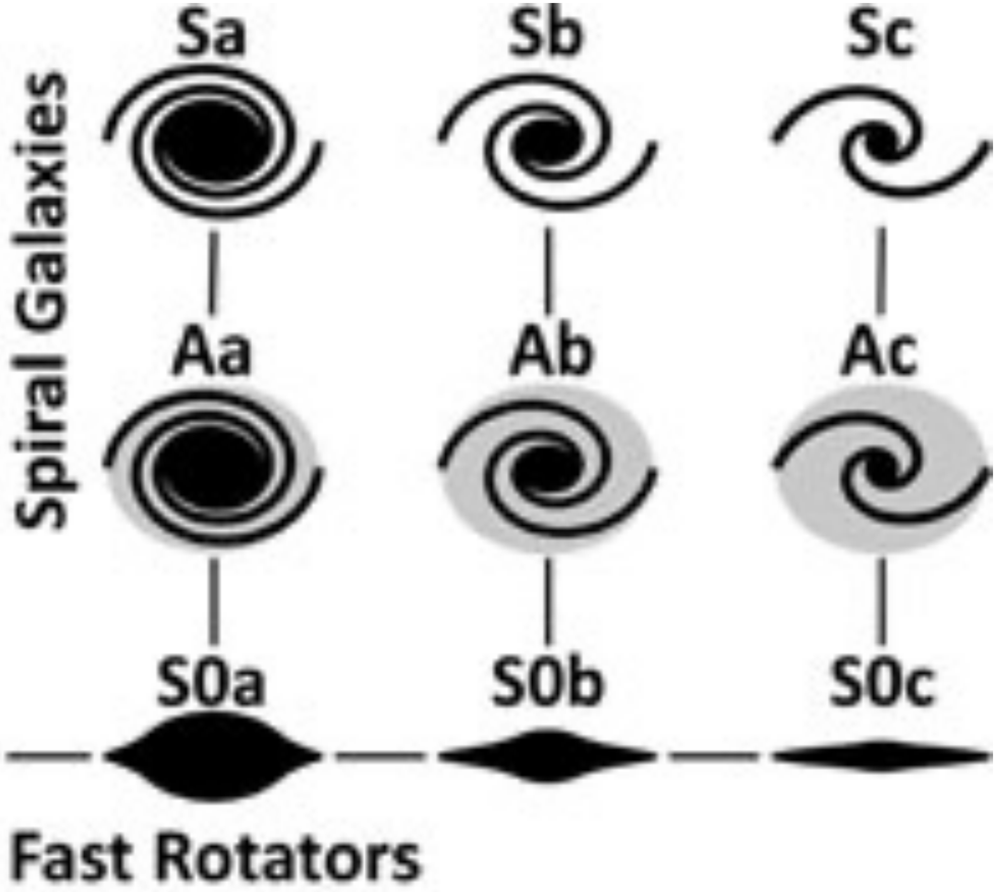

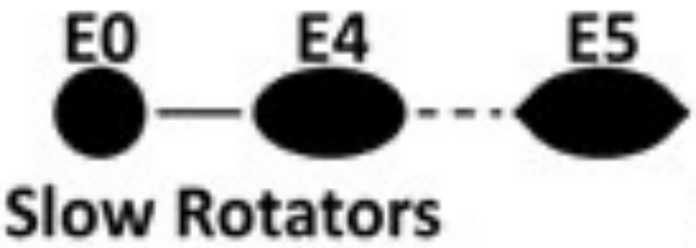

The ATLAS^{3D} comb

Galaxy Formation and Evolutions

Galaxies are believed to have formed through the merging of small galaxies and star clusters. Figure C shows large star clusters found at a distance of 5000 Mpc. They might be precursors of galaxies.

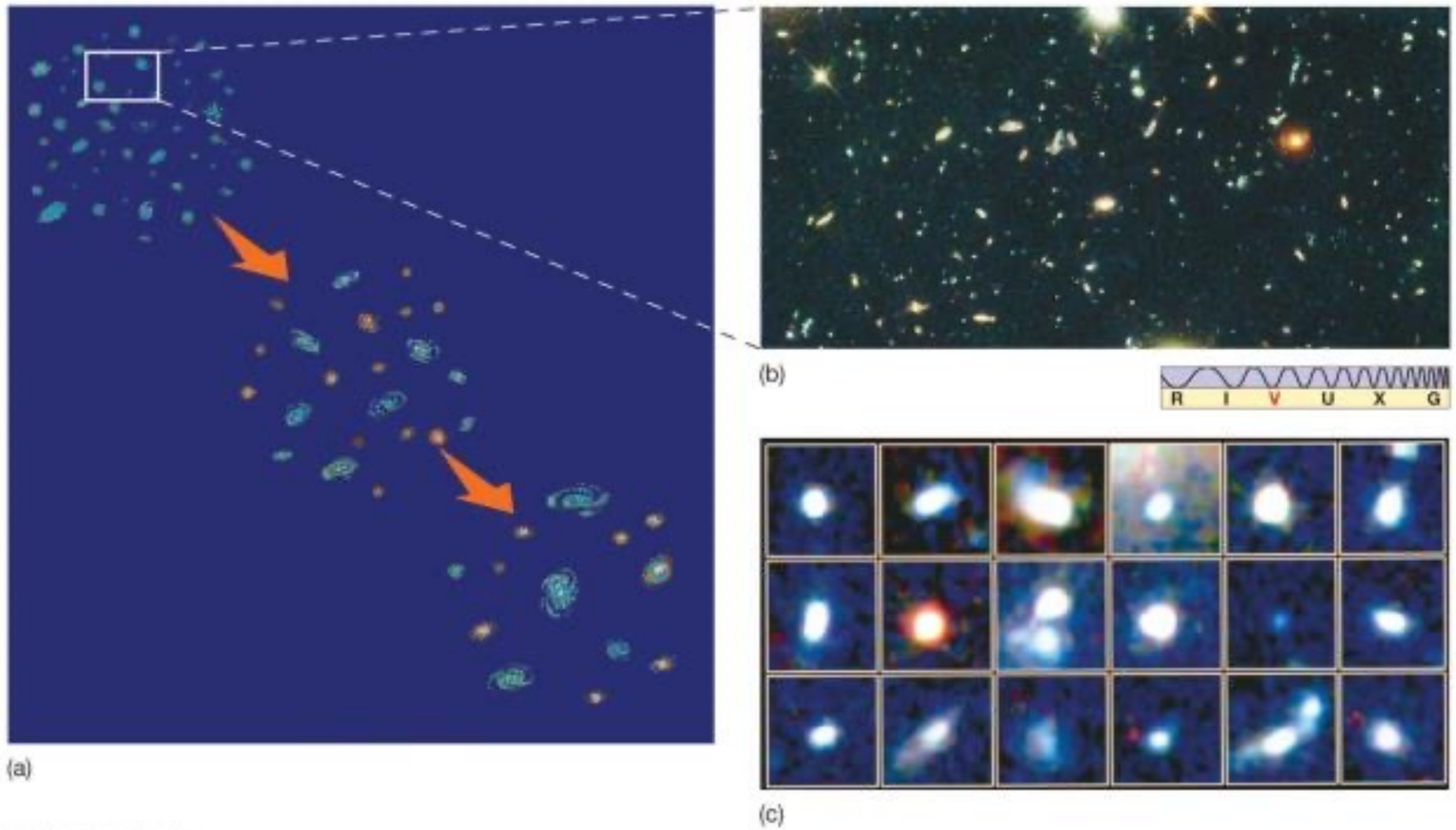

Galaxy Formation and Evolutions

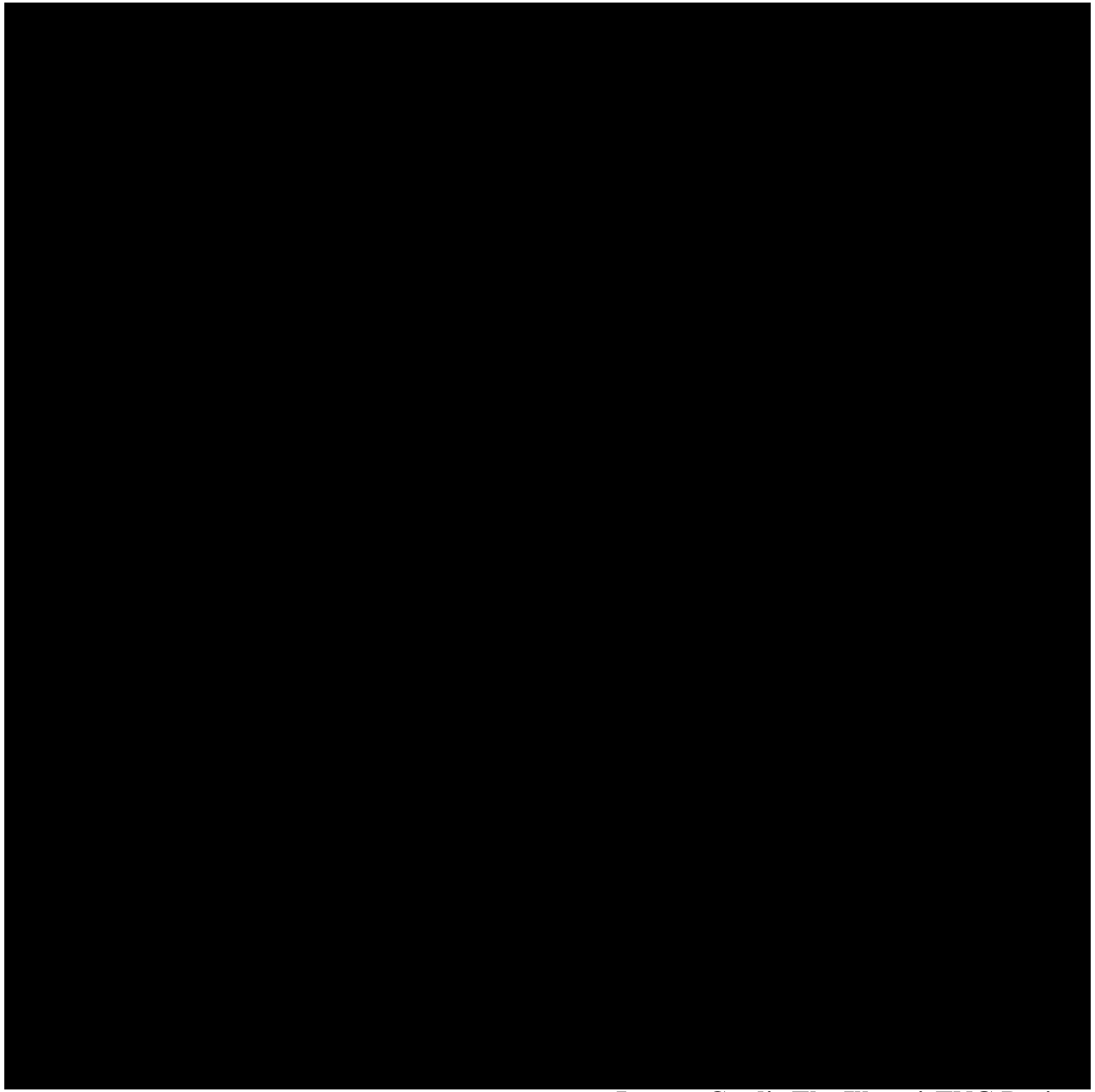

Images Credit:The IllustrisTNG Project www.tng-project.org

Gravitational Bound Systems

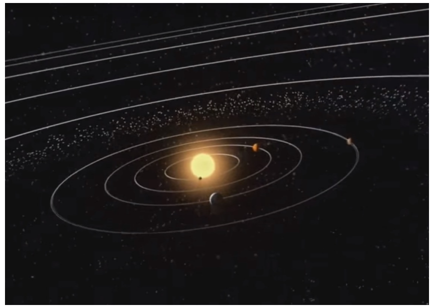

I. Solar Systems

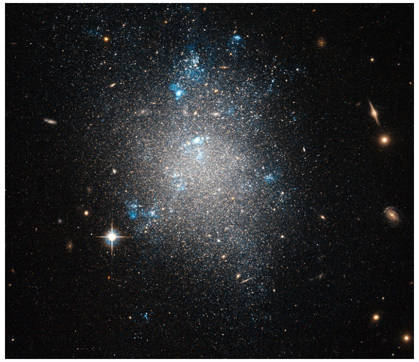

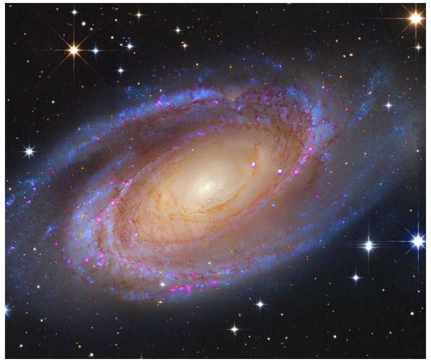

I. Galaxies
- ❖ Dwarf Galaxies
- ❖ Spiral Galaxies
- ❖ Elliptical Galaxies

II. Cluster of Galaxies (Galaxy Clusters)

Larger cosmic structures

- Superclusters
- Galaxy filaments form massive, thread-like structures on the order of millions of light-years. Computer simulation.

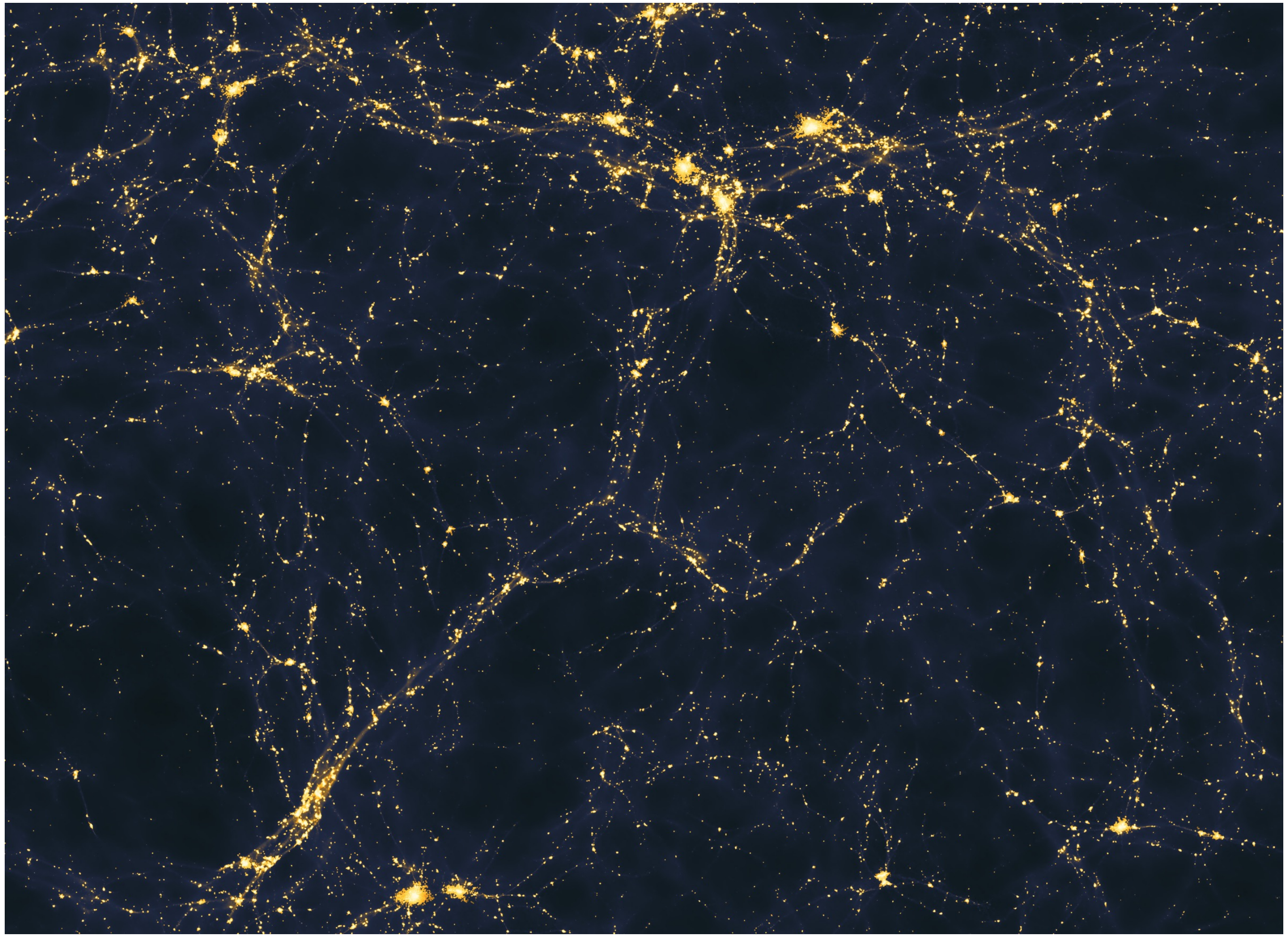

Challenges of Modern Cosmology

- **Dark Matter and Dark Energy**
- **Cosmic Microwave Background (CMB) Anomalies**
- **Hubble Tension**
- **Massive Galaxies at high redshift**

Hubble Tension

Whisker plot showing different measurements of the Hubble constant. The final measured Hubble constant of this paper was H_0 = 74.2 (the 5th line in the *Lensing related, mass model-dependent* section of this plot), which agrees with measurements from Cepheid stars, but disagrees with early Universe measurements from the CMB. [Figure 2 of Di Valentino et al. 2021]

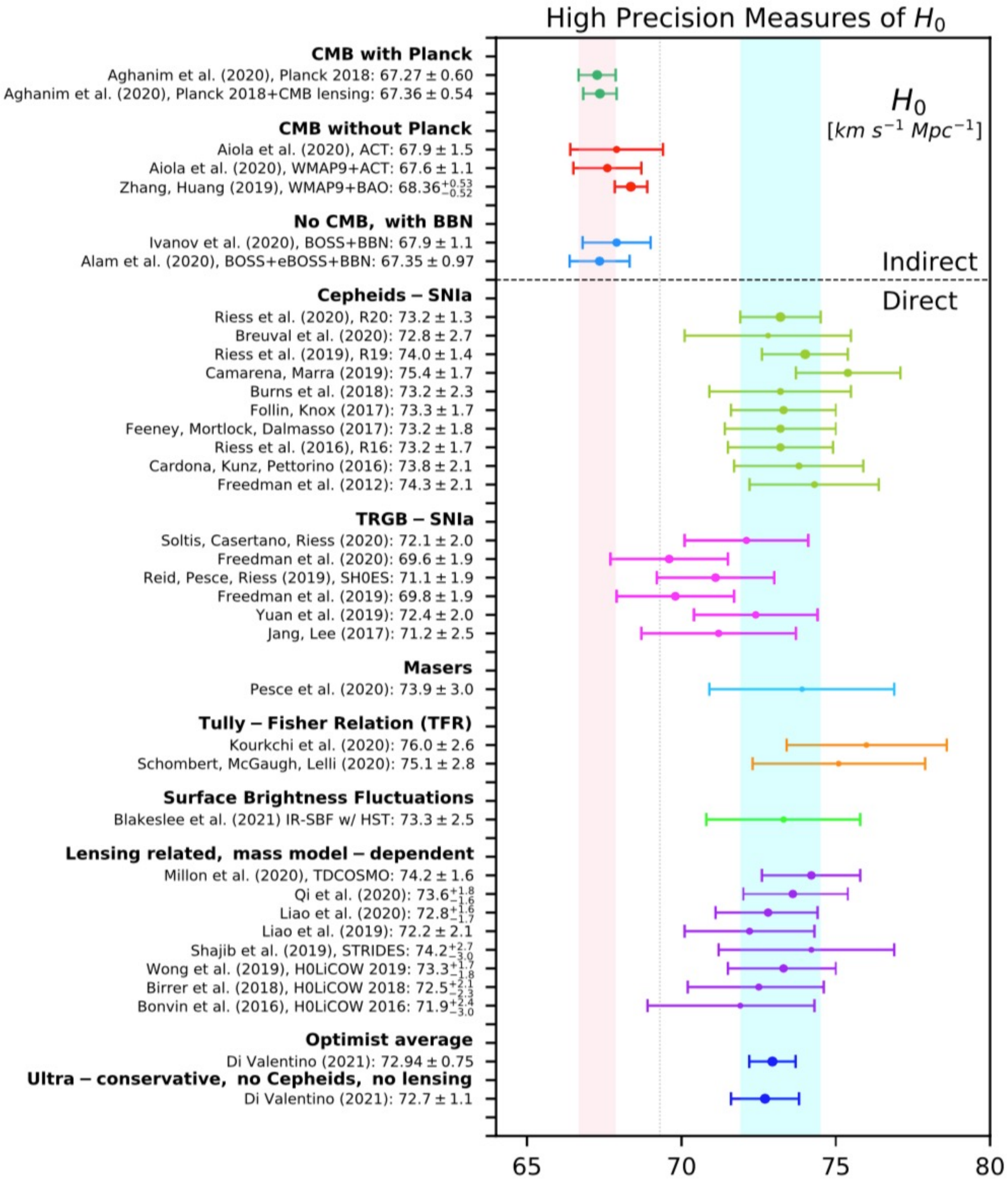

James Webb Space Telescope (JWST)

Objectives:

- Observe the universe in infrared light for breakthrough discoveries
- Study star and galaxy formation, including early galaxies
- Investigate exoplanets and their atmospheres for signs of habitability

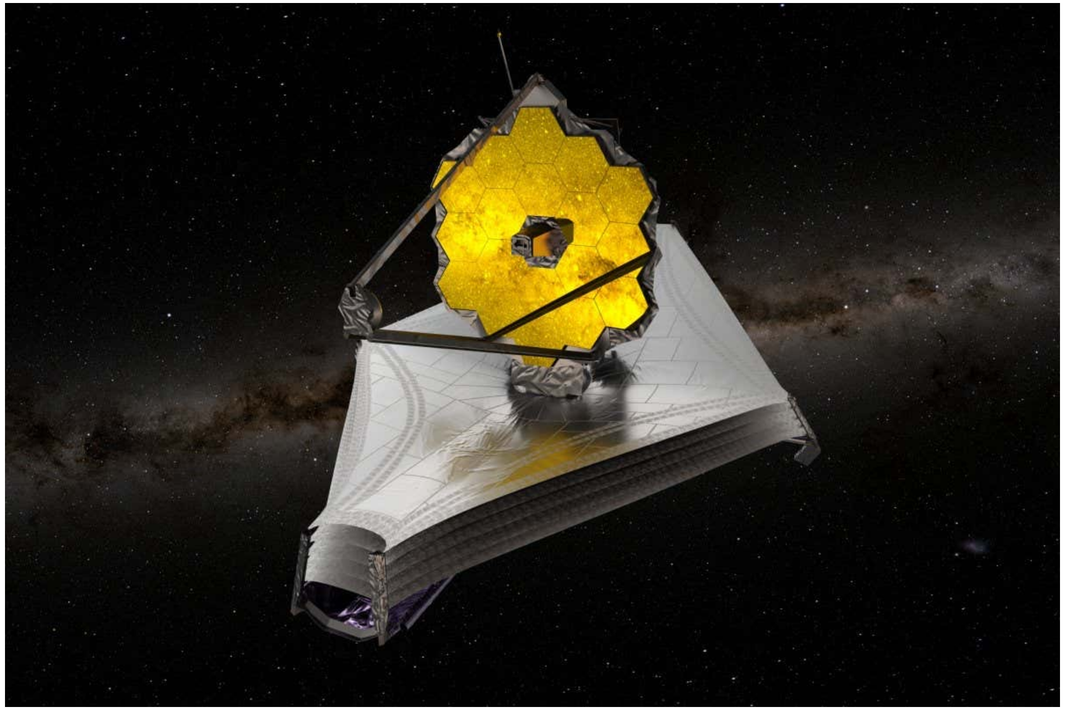

An artist's impression of the James Webb Space Telescope. ESA/ATG medialab

The Astrophysical Journal Letters, 938:L15 (9pp), 2022 October 20 https://doi.org/10.3847/2041-8213/ac94d0

Early Results from GLASS-JWST. III. Galaxy Candidates at $z \sim 9$–15*

Marco Castellano[1], Adriano Fontana[1], Tommaso Treu[2], Paola Santini[1], Emiliano Merlin[1], Nicha Leethochawalit[3,4,5], Michele Trenti[3,4], Eros Vanzella[6], Uros Mestric[6], Andrea Bonchi[7], Davide Belfiori[1], Mario Nonino[8], Diego Paris[1],

Table 1
Galaxy Candidates at $z > 9$ in GLASS-JWST-ERS[a]

ID	R.A. (deg.)	Decl. (deg.)	F444W	z_{EAzY}	z_{zphot}	M_{UV}	β	SFR ($M_\odot$ yr^{-1})	R_e (kpc)	Selection
GHZ1	3.511929	−30.371848	26.36 ± 0.05	10.53	10.63	-20.98 ± 0.06	-1.99 ± 0.10	25^{+68}_{-16}	0.43 ± 0.02	(1), (2)
GHZ2[b]	3.498985	−30.324771	27.21 ± 0.20	12.11	12.30	-21.19 ± 0.20	-3.00 ± 0.12	20^{+14}_{-13}	0.12 ± 0.01	(2)
GHZ3	3.528937	−30.363811	26.73 ± 0.07	2.69	9.33	-20.69 ± 0.09	-1.85 ± 0.17	31^{+10}_{-8}	0.88 ± 0.09	(1), (2)
GHZ4	3.513743	−30.351554	27.74 ± 0.12	10.08	9.93	-19.98 ± 0.27	-2.86 ± 0.55	5^{+19}_{-3}	0.39 ± 0.09	(1), (2)
GHZ5	3.494437	−30.307620	27.25 ± 0.08	2.49	9.20	-20.17 ± 0.18	-1.82 ± 0.33	18^{+21}_{-15}	0.21 ± 0.08	(1)
GHZ6	3.479054	−30.314925	27.43 ± 0.11	9.85	9.05	-19.66 ± 0.21	-1.67 ± 0.38	10^{+30}_{-8}	0.45 ± 0.09	photo z

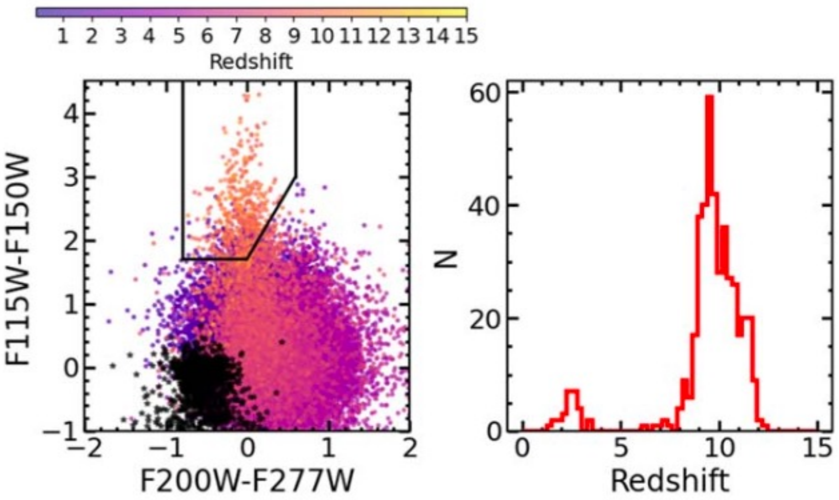

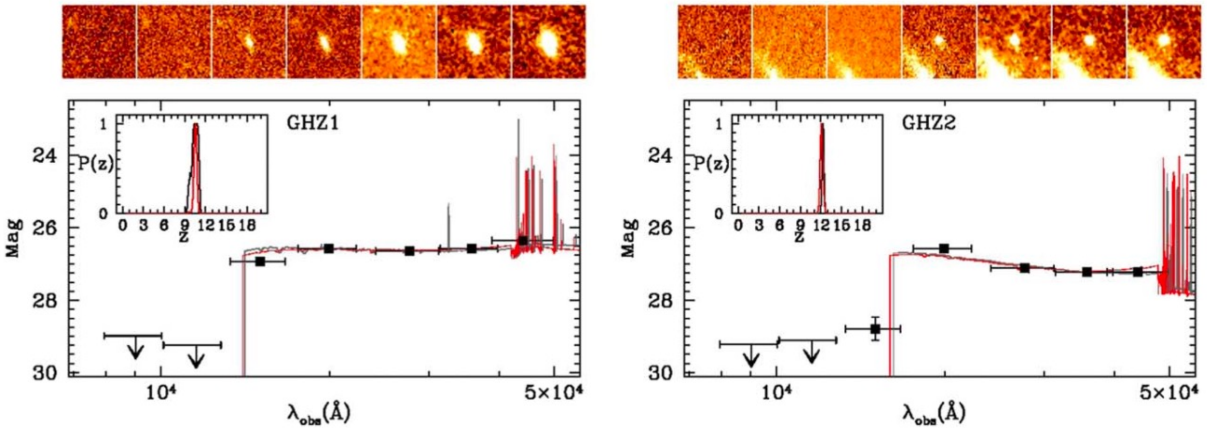

Figure 3. The two high-quality, bright high-redshift candidates from the GLASS-JWST NIRCAM field taken in parallel to NIRISS. Photometry and best-fit SEDs at the best-fit redshift are given in the main quadrant. Redshift probability distributions $P(z)$ from ZPHOT (gray) and EAZY (red) are shown in the inset. Upper limits are reported at the 2σ level, including a conservative estimate of the error budget, especially in the bluest bands (M22). Thumbnails, from left to right, show the objects in the F090W, F115W, F150W, F200W, F277W, F356W, and F444W bands.

The Astrophysical Journal Letters, 948:L14 (11pp), 2023 May 10 https://doi.org/10.3847/2041-8213/accea5

OPEN ACCESS

Early Results from GLASS-JWST. XIX. A High Density of Bright Galaxies at $z \approx 10$ in the A2744 Region

Marco Castellano[1], Adriano Fontana[1], Tommaso Treu[2], Emiliano Merlin[1], Paola Santini[1], Pietro Bergamini[3,4], Claudio Grillo[3,5], Piero Rosati[4,6], Ana Acebron[3,5], Nicha Leethochawalit[7], Diego Paris[1], Andrea Bonchi[8], Davide Belfiori[1], Antonello Calabrò[1], Matteo Correnti[1,8], Mario Nonino[9], Gianluca Polenta[8], Michele Trenti[10,11], Kristan Boyett[10,11], G. Brammer[12,13], Tom Broadhurst[14,15,16], Gabriel B. Caminha[17,18], Wenlei Chen[19], Alexei V. Filippenko[20], Flaminia Fortuni[1], Karl Glazebrook[21], Sara Mascia[1], Charlotte A. Mason[22,23], Nicola Menci[1], Massimo Meneghetti[4,24], Amata Mercurio[25,26], Benjamin Metha[2,10,11], Takahiro Morishita[27], Themiya Nanayakkara[21], Laura Pentericci[1], Guido Roberts-Borsani[2], Namrata Roy[28], Eros Vanzella[4], Benedetta Vulcani[29], Lilan Yang[30], and Xin Wang[31,32,33]

Table 3
Properties of the Galaxy Candidates at $z = 9$–11 in the GLASS-JWST, DDT, and UNCOVER Fields

ID	R.A. deg	Decl. deg	$M_{\rm UV}$ mag	$z_{\rm zphot}$	$z_{\rm EAzY-v1p3}$	$z_{\rm EAzY-Larson}$	SFR $M_\odot$ yr^{-1}	$M_{\rm star}$ $10^8\ M_\odot$	UV Slope	μ
GHZ1	3.511929	−30.371859	$-20.36^{+0.31}_{-0.19}$	$10.47^{+0.38}_{-0.89}$	$10.39^{+0.19}_{-0.20}$	$10.54^{+0.20}_{-0.19}$	$10.7^{+42.7}_{-4.7}$	$11.5^{+7.1}_{-10.3}$	-1.93 ± 0.07	$1.71^{+0.05}_{-0.05}$
GHZ4	3.513739	−30.351561	$-19.44^{+0.16}_{-0.26}$	$10.27^{+1.2}_{-1.4}$	$10.11^{+0.46}_{-0.46}$	$10.43^{+0.61}_{-0.63}$	$2.0^{+14.2}_{-0.4}$	$4.3^{+1.5}_{-3.9}$	-2.31 ± 0.36	$1.66^{+0.05}_{-0.05}$
GHZ7	3.451363	−30.320718	$-20.06^{+0.02}_{-0.17}$	$10.62^{+0.55}_{-1.02}$	$9.97^{+0.60}_{-0.32}$	$10.57^{+0.35}_{-0.33}$	$3.2^{+10.0}_{-0.5}$	$2.1^{+1.8}_{-1.7}$	-2.66 ± 0.15	$1.20^{+0.01}_{-0.01}$
GHZ8	3.451430	−30.321796	$-20.73^{+0.01}_{-0.01}$	$10.85^{+0.45}_{-0.57}$	$10.14^{+0.29}_{-0.28}$	$10.79^{+0.34}_{-0.34}$	$17.5^{+13.6}_{-12.3}$	$0.8^{+6.4}_{-0.16}$	-2.60 ± 0.14	$1.20^{+0.02}_{-0.02}$
GHZ9	3.478756	−30.345520	$-19.33^{+0.04}_{-0.12}$	$9.35^{+0.77}_{-0.35}$	$9.48^{+0.40}_{-0.37}$	$9.40^{+0.20}_{-0.22}$	$14.4^{+15.0}_{-7.3}$	$3.3^{+2.9}_{-2.4}$	-1.92 ± 0.13	$1.33^{+0.02}_{-0.02}$
DHZ1	3.617257	−30.425565	$-21.61^{+0.03}_{-0.03}$	9.3127 ± 0.0002[a]			$25.4^{+3.2}_{-4.3}$	$25^{+6.6}_{-5.0}$	-1.80 ± 0.08	$1.66^{+0.02}_{-0.01}$
UHZ1	3.567065	−30.377857	$-19.79^{+0.16}_{-0.17}$	$10.32^{+0.25}_{-1.0}$	$9.88^{+0.21}_{-0.19}$	$9.99^{+0.47}_{-0.48}$	$4.5^{+2.9}_{-2.2}$	$0.4^{+1.8}_{-0.2}$	-2.72 ± 0.15	$3.72^{+0.23}_{-0.24}$

Note. The demagnified rest frame $M_{\rm UV}$ has been obtained at the best-fit ZPHOT redshift, and the uncertainties include the contribution of both photometry and magnification. Stellar masses and SFRs have been obtained at the best-fit ZPHOT redshift as in Santini et al. (2023) and corrected for magnification. Uncertainties include error contribution from SED fitting and magnification. The UV slope β is measured by fitting the F200W, F277W, and F356W bands; the uncertainties in the fit account for photometric errors (Castellano et al. 2012). The uncertainties in the magnification μ are at the 68% confidence level; see Section 4.1.

[a] Spectroscopic redshift from Boyett et al. (2023). All properties of DHZ1 have been measured fixing the redshift at the spectroscopic value.

Massive Galaxies at high redshift

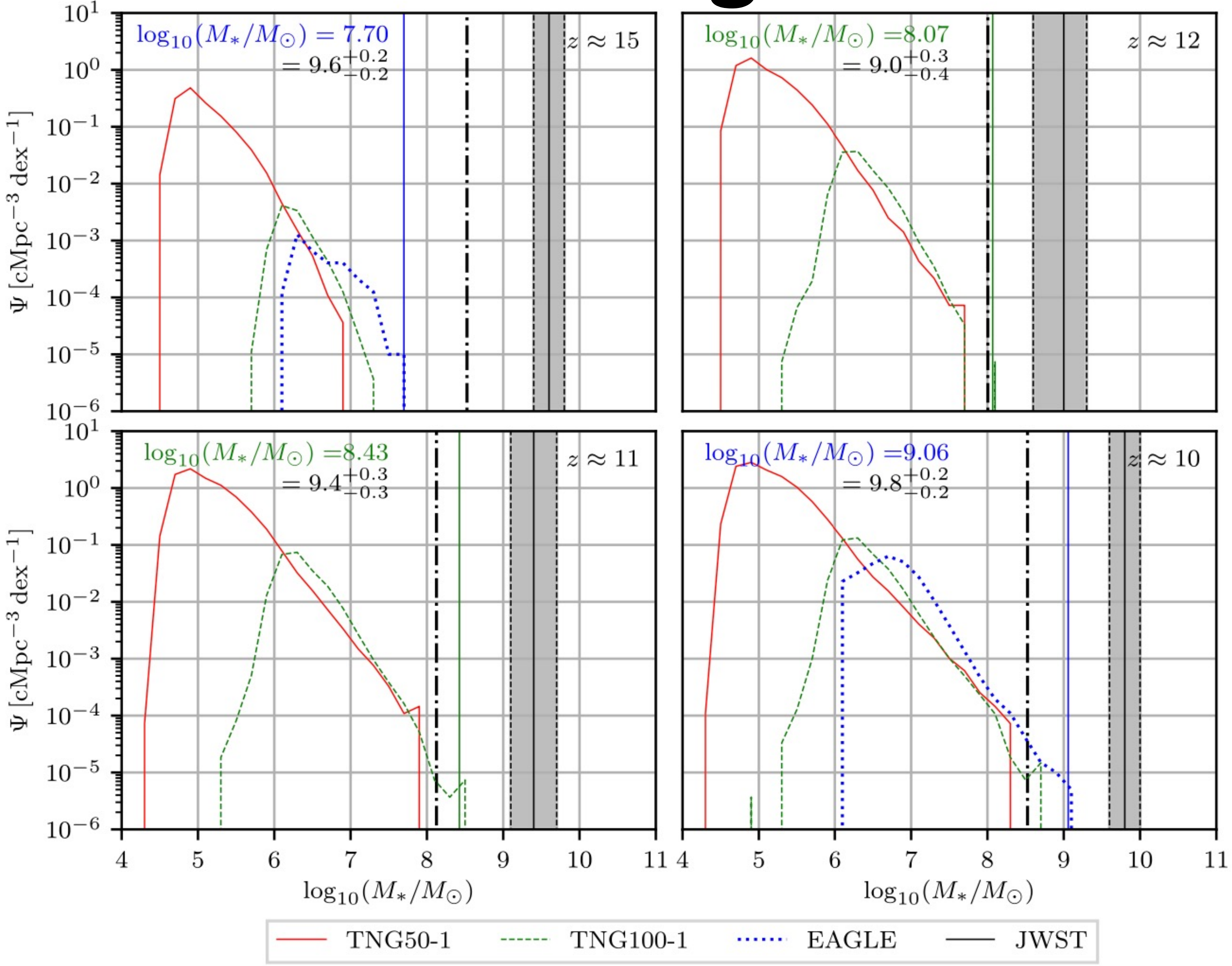

Figure 1. The GSMF at redshifts $z \approx 15$ (top left), 12 (top right), 11 (bottom left), 10 (bottom right) in the TNG50-1 (solid red), TNG100-1 (dashed green), and RefL0100N1504 (dotted blue) simulation. The colored vertical solid line marks the most massive subhalo in terms of the stellar mass in the simulations. The vertical black solid lines refer to the reported galaxy candidates CEERS-1749 (top left), GL-z13 (top right), GL-z11 (bottom left), and ID 1514 (bottom right), where the black dashed lines correspond to the measurement uncertainties. The vertical dashed–dotted lines mark the lowest possible value as inferred for different star formation histories (SFHs) in Section 3.1. The histograms are normalized by their bin width of $\Delta \log_{10}(M_*/M_\odot) = 0.2$ and volume of the simulation box.

Haslbaruer et al. (2022), ApJL, 939, L31

Euclid Space Telescope

Euclid is a pioneering space telescope mission designed to unlock the mysteries of the universe.

Launch Date: 2023/7/1

Objectives:

- Map the universe’s large-scale structure to understand the nature of dark matter and dark energy.
- Study the formation and evolution of galaxies to unravel their cosmic history.
- Investigate the properties of dark matter and dark energy to shed light on their fundamental nature.

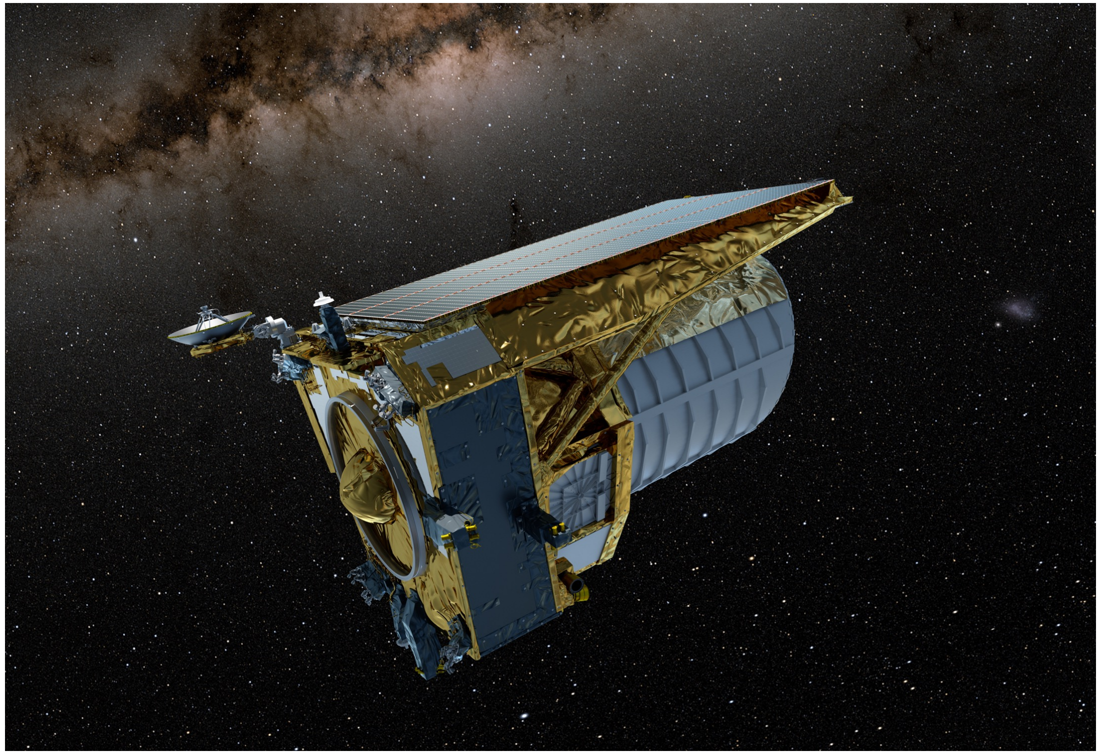

Remarks

- **Expanding universe – Hubble Law**
- **ΛCDM – CMB, Supernovae, dark matter hypothesis**
- **Bottom-up structure formation – computer simulations**
- **Challenges: CMB Anomalies, Hubble Tension, Massive Galaxies at high redshift**

Q&A

In 1927, Belgian astronomer Georges Lemaître computed a solution to Einstein's equations and discovered that the universe is constantly expanding.

In 1929, American astronomer Edwin Hubble found that galaxies further away from the Milky Way are receding faster.

Edwin Hubble
1889 - 1953

Georges Lemaître
1894 - 1966

PHYSICAL REVIEW LETTERS **127,** 161302 (2021)

Editors' Suggestion Featured in Physics

New Relativistic Theory for Modified Newtonian Dynamics

Constantinos Skordis* and Tom Złośnik†
CEICO, Institute of Physics (FZU) of the Czech Academy of Sciences, Na Slovance 1999/2, 182 21 Prague, Czech Republic

$$S = \int d^4x \frac{\sqrt{-g}}{16\pi\tilde{G}} \left[R - \frac{K_B}{2} F^{\mu\nu} F_{\mu\nu} + 2(2 - K_B) J^\mu \nabla_\mu \phi - (2 - K_B)\mathcal{Y} - \mathcal{F}(\mathcal{Y}, \mathcal{Q}) - \lambda(A^\mu A_\mu + 1) \right] + S_m[g],$$

CMB can also be explained by Relativistic MOND (RMOND)